

# Bile acid- and ethanol-mediated activation of Orai1 damages pancreatic ductal secretion in acute pancreatitis

Petra Pallagi<sup>1,2,3</sup>, Marietta Görög<sup>2,3</sup>, Noémi Papp<sup>2,3</sup>, Tamara Madácsy<sup>1,2,3</sup>, Árpád Varga<sup>1,2,3</sup> , Tim Crul<sup>1,2,3</sup> , Viktória Szabó<sup>1,2,3</sup> , Melinda Molnár<sup>2,3</sup>, Krisztina Dudás<sup>2,3</sup>, Anna Grassalkovich<sup>2</sup>, Edit Szederkényi<sup>4</sup>, György Lázár<sup>4</sup>, Viktória Venglovecz<sup>5</sup>, Péter Hegyi<sup>2,6,7</sup>  and József Maléth<sup>1,2,3</sup>

<sup>1</sup>HCEMM-SZTE Molecular Gastroenterology Research Group, University of Szeged, Szeged, Hungary

<sup>2</sup>Department of Medicine, University of Szeged, Szeged, Hungary

<sup>3</sup>ELKH-USZ Momentum Epithelial Cell Signaling and Secretion Research Group, University of Szeged, Szeged, Hungary

<sup>4</sup>Department of Surgery, University of Szeged, Szeged, Hungary

<sup>5</sup>Department of Pharmacology and Pharmacotherapy, University of Szeged, Szeged, Hungary

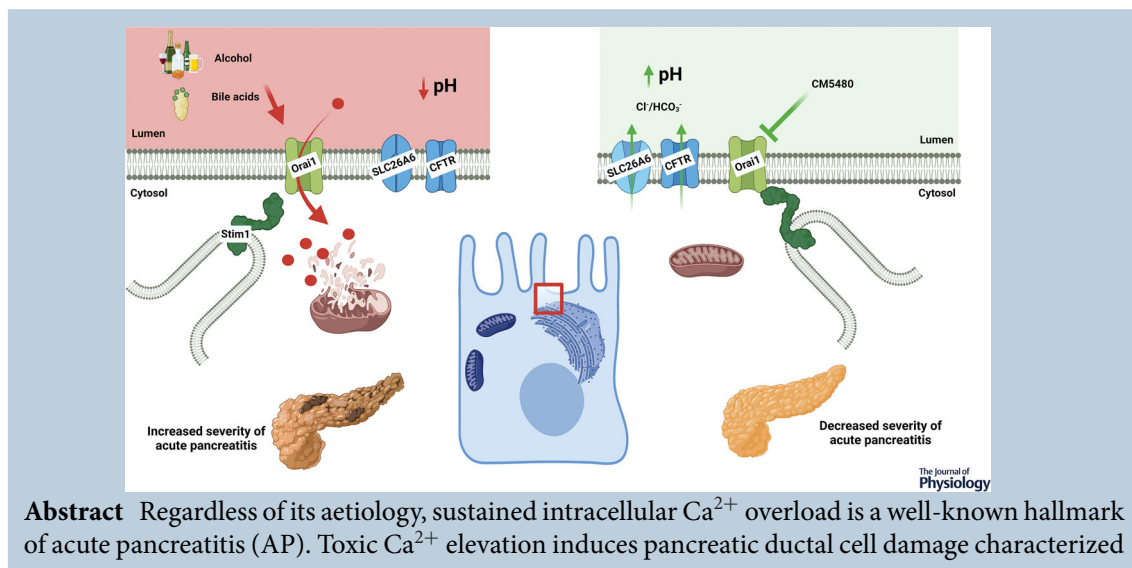
<sup>6</sup>Hungary Centre for Translational Medicine, Semmelweis University, Budapest, Hungary

<sup>7</sup>Institute for Translational Medicine and First Department Medicine, Medical School, University of Pécs, Pécs, Hungary

Edited by: Kim Barrett & Pawel Ferdek

Linked articles: This article is highlighted in a Perspectives article by Gerasimenko & Gerasimenko. To read this article, visit <https://doi.org/10.1113/JP282826>.

The peer review history is available in the Supporting Information section of this article (<https://doi.org/10.1113/JP282203#support-information-section>).



**Petra Pallagi** is a research fellow at the First Department of Internal Medicine at the University of Szeged. She earned her PhD under the supervision of Peter Hegyi and Zoltan Rakonczay at the University of Szeged for her work on the role of pancreatic ductal secretion in acute pancreatitis pathogenesis. She also investigated how activated trypsin inhibits pancreatic ductal secretion. Her current work focuses on the intracellular signalling and secretion in the exocrine pancreas. **Marietta Görög** is a PhD candidate at the University of Szeged, Internal Medicine and supervised by Dr József Maléth and Dr Pallagi Petra. She holds a MSc degree in Biology, specialized in molecular biology. Currently, her research focuses on understanding the role of  $\text{Ca}^{2+}$  signalling in the physiology and pathophysiology of the pancreatic ductal cells. She found that Orai1 inhibition prevents acute pancreatitis-related ductal cell function impairment.



P. Pallagi and M. Görög contributed equally to this work.

by impaired ion and fluid secretion – essential to wash out the protein-rich fluid secreted by acinar cells while maintaining the alkaline intra-ductal pH under physiological conditions – and mitochondrial dysfunction. While prevention of ductal cell injury decreases the severity of AP, no specific drug target has yet been identified in the ductal cells. Although Orai1, a store-operated  $\text{Ca}^{2+}$  influx channel, is known to contribute to sustained  $\text{Ca}^{2+}$  overload in acinar cells, details concerning its expression and function in ductal cells are currently lacking. In this study, we demonstrate that functionally active Orai1 channels reside predominantly in the apical plasma membrane of pancreatic ductal cells. Selective CM5480-mediated Orai1 inhibition impairs Stim1-dependent extracellular  $\text{Ca}^{2+}$  influx evoked by bile acids or ethanol combined with non-oxidative ethanol metabolites. Furthermore, prevention of sustained extracellular  $\text{Ca}^{2+}$  influx protects ductal cell secretory function *in vitro* and decreases pancreatic ductal cell death. Finally, Orai1 inhibition partially restores and maintains proper exocrine pancreatic secretion in *in vivo* AP models. In conclusion, our results indicate that Orai1 inhibition prevents AP-related ductal cell function impairment and holds the potential of improving disease outcome.

(Received 2 August 2021; accepted after revision 21 December 2021; first published online 26 January 2022)

**Corresponding author** J. Maléth: HAS-USZ Momentum Epithelial Cell Signaling and Secretion Research Group, First Department of Internal Medicine and Department of Public Health, University of Szeged, H6720, Szeged, Hungary. Email: jozsefmaeth1@gmail.com; maleth.jozsef@med.u-szeged-hu

**Abstract figure legend** Alcohol and bile acids induce Orai1 mediated extracellular  $\text{Ca}^{2+}$  entry in pancreatic ductal cells leading to cell damage. The inhibition of Orai1 during acute pancreatitis improves pancreatic ductal cell function.

### Key points

- Sustained intracellular  $\text{Ca}^{2+}$  overload in pancreatic acinar and ductal cells is a hallmark of biliary and alcohol-induced acute pancreatitis, which leads to impaired ductal ion and fluid secretion.
- Orai1 is a plasma membrane  $\text{Ca}^{2+}$  channel that mediates extracellular  $\text{Ca}^{2+}$  influx upon endoplasmic reticulum  $\text{Ca}^{2+}$  depletion.
- Results showed that Orai1 is expressed on the luminal plasma membrane of the ductal cells and selective Orai1 inhibition impaired Stim1-dependent extracellular  $\text{Ca}^{2+}$  influx evoked by bile acids or ethanol combined with non-oxidative ethanol metabolites.
- The prevention of sustained extracellular  $\text{Ca}^{2+}$  influx protected ductal cell secretory functions in *in vitro* models and maintained exocrine pancreatic secretion in *in vivo* acute pancreatitis models.
- Orai1 inhibition prevents the bile acid- and alcohol-induced damage of the pancreatic ductal secretion and holds the potential of improving the outcome of acute pancreatitis.

## Introduction

Acute pancreatitis (AP) is one of the most common inflammatory diseases of the gastrointestinal tract that require hospitalization. It is primarily caused by impacted gallstones, heavy alcohol consumption, hypertriglyceridaemia or through iatrogenic side effects of medical treatments such as asparaginase or endoscopic retrograde cholangiopancreatography (ERCP), thus representing a major clinical challenge (Yadav & Lowenfels, 2013). Despite advances in basic and clinical research, specific treatments are still lacking, resulting in a remarkably high mortality rate (~28%) in cases of severe AP (~10% of all cases) (Párniczky *et al.* 2016). Previously, a crucial involvement of impaired ductal secretion in AP development was shown. Our group demonstrated

ethanol+fatty acid-induced reductions in expression and activity of cystic fibrosis transmembrane conductance regulator (CFTR) in pancreatic ductal epithelial cells in a mouse model of alcohol-induced AP, ultimately leading to impaired ductal secretion and increased severity of the disease (Maléth *et al.* 2015). Also, mislocalization of CFTR in mice lacking the  $\text{Na}^+/\text{H}^+$  exchanger regulatory factor-1 (NHERF1) – a scaffolding protein that targets membrane proteins to the apical membrane – resulted in decreased ductal secretion and more severe experimental AP (Pallagi *et al.* 2014). Notably, dysfunction of ductal epithelia equally damages acinar cells. Freedman *et al.* (2001) showed disturbed plasma membrane (PM) dynamics and apical endocytosis in pancreatic acini of CFTR knockout mice. Importantly, pharmacological restoration of CFTR-mediated secretion with the corrector C18 and

the potentiator VX-770 restored acinar cell function and decreased pancreatic inflammation in mouse models of chronic and autoimmune pancreatitis (Zeng *et al.* 2017). Proper establishment of an alkaline intraductal pH environment prevents premature intra-pancreatic, acidic pH-dependent autoactivation of trypsinogen (Pallagi *et al.* 2011).

Regardless of the aetiology, different forms of AP are characterized by a sustained intracellular  $\text{Ca}^{2+}$  elevation (Pallagi *et al.* 2020). Biologically active compounds, such as bile acids and fatty acid ethyl esters, induce the release of  $\text{Ca}^{2+}$  from endoplasmic reticulum (ER)  $\text{Ca}^{2+}$  stores and subsequent extracellular  $\text{Ca}^{2+}$  influx through the Orai1  $\text{Ca}^{2+}$  channel, a process referred to as store-operated  $\text{Ca}^{2+}$  entry (SOCE). Although SOCE is part of the physiological  $\text{Ca}^{2+}$  signalling events in non-excitabile cells, it can significantly contribute to sustained intracellular  $\text{Ca}^{2+}$  overload under pathological conditions. In addition, ERCP-mediated intra-pancreatic pressure increase leads to extracellular  $\text{Ca}^{2+}$  influx through the activation of TRPV4 and the mechanoreceptor ion channel Piezo1 (Swain *et al.* 2020). Intracellular  $\text{Ca}^{2+}$  overload leads to premature activation of trypsinogen in pancreatic acinar cells (Krüger *et al.* 2000) as well as mitochondrial damage and cell necrosis in pancreatic ductal cells (Criddle *et al.* 2006). Based on our previous observations – indicating sustained intracellular  $\text{Ca}^{2+}$  elevation-mediated impairment of fluid and  $\text{HCO}_3^-$  secretion (Maléth & Hegyi, 2014; Madácsy *et al.* 2018) as well as ductal cell mitochondrial malfunctioning, subsequent ATP depletion and cell damage (Maléth *et al.* 2011) – we hypothesize that extracellular  $\text{Ca}^{2+}$  influx might contribute to disease development through establishment of a persistent alcohol- or fatty acid esters (FAEEs)-induced intracellular  $\text{Ca}^{2+}$  increase resulting in impaired mitochondrial ATP production. Subsequently, this leads to failing ATP-dependent  $\text{Ca}^{2+}$  extrusion by the plasma membrane  $\text{Ca}^{2+}$ -ATPase and  $\text{Ca}^{2+}$  reuptake by the sarco/endoplasmic reticulum  $\text{Ca}^{2+}$ -ATPase (Kim *et al.* 2002) thus maintaining the spatiotemporal localization of the  $\text{Ca}^{2+}$  signal and developing a global, sustained  $\text{Ca}^{2+}$  elevation. Selective inhibition of Orai1 by GSK-7975A or CM-128 (also known as CM4620 or Auxora, developed by CalciMedica) markedly impaired bile acid-mediated extracellular  $\text{Ca}^{2+}$  influx and sustained  $\text{Ca}^{2+}$  overload in pancreatic acinar cells and decreased AP severity in experimental models (Wen *et al.* 2015). Moreover, selective inhibition of Orai1 by CM4620 abolished myeloperoxidase activity and inflammatory cytokine expression in pancreatic and lung tissues and prevented oxidative burst in neutrophils (Waldron *et al.* 2019). Based on these preclinical observations, CalciMedica successfully completed two phase I clinical trials and then tested seven patients with AP to assess the pharmacokinetic and pharmacodynamics profile

of Auxora when administered by intravenous infusion. Based on these, a phase 2 open-label, dose–response clinical study evaluated the safety of Auxora in patients with AP, systemic inflammatory response syndrome (SIRS) and hypoxaemia (Brien *et al.* 2021). While low-dose Auxora treatment improved moderate to mild AP in 36.5% of the patients, very interestingly Auxora also improved the tolerance of solid foods, which might be explained by improved exocrine pancreatic secretion. Although the beneficial effect of selective Orai1 inhibition in AP is well-established, precisely how Orai1 inhibition affects pancreatic ductal secretion is unknown.

Therefore, in this study, we aimed to analyse the effect of Orai1 inhibition on ductal secretion in isolated ductal fragments, pancreatic organoids and *in vivo* AP models. Our results demonstrate that selective inhibition of Orai1 by CM5480, another CalciMedica selective Orai1 channel inhibitor, impairs Stim1-dependent extracellular  $\text{Ca}^{2+}$  influx evoked by bile acids or ethanol combined with non-oxidative ethanol metabolites. Furthermore, prevention of sustained extracellular  $\text{Ca}^{2+}$  influx protects ductal cell secretory function *in vitro* and decreases pancreatic ductal cell death. Finally, Orai1 inhibition partially restores and maintains exocrine pancreatic secretion in *in vivo* AP models. In conclusion, our results indicate that Orai1 inhibition prevents AP-related impairment of ductal cell function and holds the potential of improving disease outcome.

## Methods

### Ethics

Animals were used with adherence to the NIH guidelines and the EU directive 2010/63/EU. The study was approved by the National Scientific Ethical Committee on Animal Experimentation under licence number XXI/1541/2020. The collection and use of human samples including cadaver donor pancreas and liver samples were carried out in adherence with the EU standards and approved by the Regional Committee of Research Ethics of the Hungarian Medical Research Council under licence number 37/2017-SZTE.

### Animals

FVB/N mice (8–12 weeks, 20–25 g) were kept at constant room temperature of 22–24°C under a 12 h light–dark cycle with free access to food and water. For all experimental groups, the sex ratio was 1:1. Animals used in the experiments were bred in the animal facility of the Department of Public Health, University of Szeged. Animals received VRF1(P) standard rodent food (cat. no. 801900, Special Diets Services) and standard bedding (JRS REHOFIX MK2000 corn cob), purchased from Akromom

(Budapest, Hungary). Interventions were made during the light cycle and animals were not fasted before the experiments.

### Isolation of pancreatic ductal fragments

Pancreatic ductal fragments were isolated as described earlier (Maléth *et al.* 2015). Briefly, following pentobarbital-induced terminal anaesthesia, the pancreas was surgically removed, placed into ice-cold Dulbecco's modified Eagle's medium (DMEM)/F12, and injected with a solution containing 100 U ml<sup>-1</sup> collagenase, 0.1 mg ml<sup>-1</sup> trypsin inhibitor, 1 mg ml<sup>-1</sup> bovine serum albumin followed by shaking at 37°C for 30 min. Next, small intra- and interlobular ducts were identified and isolated under a stereomicroscope.

### Mouse and human organoid cultures

Organoid cultures (OCs) were established as previously described (Boj *et al.* 2015; Molnár *et al.* 2020; Breunig *et al.* 2021) with some modifications. Human pancreatic OCs were generated from cadaver donor-derived pancreatic tissue samples (ethical approval no.: 37/2017-SZTE). Mouse and human tissues were minced into small fragments and depending on tissue stiffness incubated for 30 min up to 1 h in digestion solution on a vertical shaker at 37°C. Next, cells were collected, washed twice and mixed with Matrigel in a 1/5 ratio. OCs were maintained in feeding medium, which was changed every other day. For passaging, OCs were incubated with TrypLE™ Express Enzyme (Thermo Fisher Scientific, Waltham, Massachusetts, USA) at 37°C for 15 min on a vertical shaker, after which the resulting cells were washed and plated in Matrigel. Details of materials and solutions used can be found in Tables 1–5.

### Gene expression analysis and gene knockdown

Total mRNA from acini and ductal fragments was purified with NucleoSpin RNA XS kit according to the manufacturer's instructions. One microgram of mRNA was used to synthesize cDNA with iScript cDNA Synthesis kit (Bio-Rad Laboratories, Hercules, CA, USA; cat. no. 1708890). Conventional PCR amplification was performed with DreamTaq Hot Start DNA Polymerase and cDNA-specific Orail primers (forward: 5'-CTTCGCCATGGTAGCGAT-3'; reverse: 5'-TGTGGTGCAGGCACTAAAGA-3') for 35 cycles. For gene knockdown studies, isolated mouse ductal fragments were transfected with 50 nM pre-designed siRNA for mouse Stim1 (Table 1) or siGLOGreen transfection indicator with Lipofectamine 2000 (ThermoFisher Scientific, Waltham, Massachusetts, USA) in feeding medium for 24 h.

**Table 1. List of materials**

Name	Manufacturer	Cat. no.
DMEM/F12	Sigma-Aldrich	D6421
Collagenase	Worthington	LS005273
Trypsin inhibitor	Thermo Fisher Scientific	17075029
Bovine serum albumin	Sigma-Aldrich	A8022
TrypLE™ Express	Thermo Fisher Scientific	12605028
Shandon Cryomatrix	ThermoFisher Scientific	6769006
Anti-Orail (extracellular) antibody	Alomone Labs	ACC-062
Goat anti-rabbit IgG (H+L) highly cross-adsorbed secondary antibody, Alexa Fluor 488	Thermo Fisher Scientific	A-11034
Hoechst33342	Thermo Fisher Scientific	62249
Fluoromount	Sigma Aldrich	F4680
Fura-2 AM	Thermo Fisher Scientific	F1201
MQAE	Thermo Fisher Scientific	E3101
BCECF AM	Thermo Fisher Scientific	B1170
Poly-L-lysine	Sigma-Aldrich	P4707-50ML
Coverglass	VWR	ECN 631–1583
Fluo4	Thermo Fisher Scientific	50018
Palmitoleic acid	Sigma-Aldrich	P9417
NucleoSpin RNA XS kit	Macherey-Nagel	740902.50
iScript cDNA Synthesis kit	Bio-Rad Laboratories	1708890
DreamTaq Hot Start DNA polymerase	Thermo Fisher Scientific	EP1702
ON-TARGETplus Mouse siRNA, SMARTpool mouse STIM1	Dharmacon	L-062376-00-0005
siGlo Green transfection indicator	Dharmacon	D-001630-01-05
Cerulein	Bachem	H-3220
Na-taurocholate	Sigma-Aldrich	86339
Secretin	Sigma-Aldrich	57147
Cyclopiazonic acid	Tocris	1235
Chenodeoxycholate	Sigma-Aldrich	C9377
Palmitic acid	Sigma-Aldrich	P0500
Paraformaldehyde	Alfa Aesar	43368
CELLview™ slide	Greiner Bio-One	543079
Apoptosis/necrosis detection assay	Abcam	ab176749
Cultrex Ultramatrix	Bio-Techne	BME001-01

**Table 2. Composition of solutions used during experiments**

	Standard HEPES	Ca-free HEPES	Standard HCO <sub>3</sub> <sup>-</sup>	NH <sub>4</sub> Cl-HCO <sub>3</sub> <sup>-</sup>	Cl <sup>-</sup> -free HCO <sub>3</sub> <sup>-</sup>
NaCl	130	132	115	95	
KCl	5	5	5	5	
MgCl <sub>2</sub>	1	1	1	1	
CaCl <sub>2</sub>	1		1	1	
HEPES	10	10			
Glucose	10	10	10	10	10
NaHCO <sub>3</sub> <sup>-</sup>			25	25	25
EGTA		0.1			
NH <sub>4</sub> Cl				20	
Na-gluconate					115
K <sub>2</sub> -sulphate					2.5
Ca-gluconate					6
Mg-gluconate					1

**Table 3. Splitting medium**

Component	Manufacturer, cat. no.	Final volume
Advanced DMEM/F-12	Thermo Fisher Scientific, 12634-010	500 ml
1 M HEPES	Thermo Fisher Scientific, 15630080	5 ml (10 mM)
GlutaMax supplement (100×)	Thermo Fisher Scientific, 35050061	5ml (1×)
Primocin (400×)	Thermo Fisher Scientific, ant-pm-2	1.25 ml (1×)

**Table 4. Digestion medium**

Component	Manufacturer, cat. no.	Final volume
Splitting medium	—	20 ml
Collagenase IV	Worthington, LS004188	1250 U ml <sup>-1</sup>
Dispase	Sigma-Aldrich, D4693-1G	0.5 U ml <sup>-1</sup>
FBS	Thermo Fisher Scientific, 10500064	0.5 ml 2.5% v/v
Trypsin inhibitor	Sigma-Aldrich, Catalog No: T9128-1G	1 mg ml <sup>-1</sup>

**Table 5. Wash medium**

Component	Manufacturer, cat. no.	Final volume
Splitting medium	—	—
Fetal bovine serum	Thermo Fisher Scientific, 10500064	2.5% v/v
Antibiotic-antimycotic solution (100×)	Thermo Fisher Scientific, 15240062	1×
Kanamycin sulfate (100×)	Thermo Fisher Scientific, 15160047	1×
Voriconazole	Tocris, 3760/10	2 µg ml <sup>-1</sup>

### Immunofluorescence labelling

Upon freezing in Shandon Cryomatrix, isolated pancreatic ducts were sectioned and stained as previously described (Molnár *et al.* 2020). Briefly, sections

were fixed in 4% paraformaldehyde for 15 min, washed 3 times in Tris-buffered saline (TBS), and blocked for 1 h with 0.1% goat serum and 10% BSA in TBS. Next, sections were incubated with anti-Orai1 antibody for

16 h at 4°C followed by incubation with anti-rabbit antibody conjugated with Alexa Fluor 488 for 2 h at room temperature. Nuclei were visualized through staining with 1  $\mu\text{g ml}^{-1}$  Hoechst33342 for 15 min after which sections were mounted with Fluoromount. Images were captured with a Zeiss LSM880 confocal microscope (Carl Zeiss Microscopy, Oberkochen, Germany) using a  $\times 40$  oil immersion objective (Zeiss, NA: 1.4).

### Measurement of intracellular $\text{Ca}^{2+}$ , $\text{Cl}^-$ , pH and mitochondrial potential by fluorescence microscopy

Intracellular  $\text{Ca}^{2+}$  concentration ( $[\text{Ca}^{2+}]_i$ ), intracellular  $\text{Cl}^-$  ( $[\text{Cl}]_i$ ) and intracellular pH ( $\text{pH}_i$ ) were measured as described previously (Molnár *et al.* 2020) by loading the cells with Fura-2-AM (2  $\mu\text{mol l}^{-1}$ ), MQAE (2  $\mu\text{mol l}^{-1}$ ) or BCECF-AM (1  $\mu\text{mol l}^{-1}$ ), respectively. Ducts or organoids were attached to a poly-L-lysine-coated coverslip and mounted on an Olympus IX71 fluorescence microscope (Olympus, Tokyo, Japan) equipped with an MT-20 illumination system. Filter sets used for Fura2, MQAE and BCECF measurements were described previously (Molnár *et al.* 2020). The signal was captured by a Hamamatsu ORCA Flash 4.0 V3 CMOS camera (Hamamatsu Photonics, Hamamatsu, Japan) through a  $\times 20$  oil immersion objective (Olympus; NA: 0.8) with a temporal resolution of 1 s. Ratiometric image analysis for  $\text{pH}_i$  measurements was performed by Olympus Excellence software. Fluorescence signals of Fura2- and MQAE-loaded samples were normalized and represented as  $F_1/F_0$  values.

### Apoptosis/necrosis detection assay

Mouse pancreatic ductal organoids were attached on a CELLview<sup>TM</sup> slide pre-coated with poly-L-lysine. Organoids were treated with either 250  $\mu\text{M}$  chenodeoxycholate (CDC) or 100 mM ethanol (EtOH) and 200  $\mu\text{M}$  palmitic acid (PA) for 30 min; CM5480 groups were treated with 10  $\mu\text{M}$  CM5480 simultaneously with CDC or EtOH+PA treatment prior to the assay. An apoptosis/necrosis detection assay was carried out according to the manufacturer's (Abcam, Cambridge, UK) protocol (Fanczal *et al.* 2020). Briefly, organoids were washed twice with assay buffer, resuspended in a mixture containing 100 $\times$  diluted Apopxin Green, 200 $\times$  diluted 7-Aminoactinomycin D (7-AAD), and 200 $\times$  diluted Cytocalcein 450 in assay buffer. Organoids were incubated in the concoction for 30 min at 37°C in a humidified incubator. Next, organoids were washed twice in fresh assay buffer and visualized in fresh assay buffer by a Zeiss LSM 880 confocal microscope at  $E_x/E_m = 490/525$  nm for Apopxin Green,  $E_x/E_m = 550/650$  nm for

7-AAD and  $E_x/E_m = 405/450$  nm for Cytocalcein Violet 450.

### Cell viability assay

Mouse pancreatic ductal organoids were grown in Cultrex Ultramatrix until passage number 3. Organoid domes were transferred into 96-well Lumitrac microplate (Greiner, 655075, Kremsmünster, Austria) and treated in 100  $\mu\text{l}$  cell culture medium for 30 min at 37°C in a humidified incubator. CellTiter-Glo 3D cell viability assay (Promega Corp., G9681, Madison, WI, USA) was carried out according to the manufacturer's protocol. Briefly, a volume of CellTiter-Glo 3D reagent was added equal to the volume of each well. Contents were mixed for 5 min in CLARIOstar Plus plate reader (BMG Labtech, Ortenberg, Germany). The plate was allowed to incubate at room temperature for an additional 25 min. Luminescence was recorded in a CLARIOstar Plus plate reader. Total protein amount was determined using by Bradford assay in a spectrophotometer (Thermo Scientific NanoDrop One). Blank corrected data were normalized to the total protein amount.

### In vivo acute pancreatitis models

In the cerulein-induced AP model, AP mice received seven hourly injections of cerulein (50  $\mu\text{g kg}^{-1}$ , I.P.) whereas control animals received injections containing physiological saline (I.P.) solution. One hour after the first cerulein injection, CM5840 (20  $\text{mg kg}^{-1}$ , I.P.) was administered. Twelve hours after the first cerulein injection, mice were sacrificed with pentobarbital (85  $\text{mg kg}^{-1}$ , I.P.).

Biliary AP was induced by intraductal administration of 4% sodium taurocholate (Na-TC) as previously described by Perides *et al.* (2010). Briefly, mice were anaesthetized with a ketamine and xylazine (respectively 125 and 12.5  $\text{mg kg}^{-1}$ , I.P.) cocktail followed by median laparotomy, the common biliopancreatic duct was cannulated across the duodenum with a 0.4 mm diameter needle connected to an infusion catheter, and the bile duct was occluded with a microvessel clip. Next, the mice received 2  $\mu\text{l g}^{-1}$  of 4% Na-TC or physiological saline at a perfusion rate of 10  $\mu\text{l min}^{-1}$  (TSE System GmbH, Berlin, Germany). Following the infusion, the abdominal wall and skin were closed separately, and the mice were placed on a heating pad until waking while buprenorphine (0.075  $\text{mg kg}^{-1}$ , I.P.) was administered to relieve the pain. One hour after the 4% Na-TC infusion, the animals received CM5480 (20  $\text{mg kg}^{-1}$ , I.P.). Directly after recovery from anaesthesia and 12 h after the operation, the mice received 0.1  $\text{mg kg}^{-1}$  buprenorphine. Twenty-four hours after the operation, the mice were

anaesthetized with pentobarbital (85 mg kg<sup>-1</sup>, i.p.) and sacrificed through exsanguination through the heart.

The mouse model of acute alcohol-induced pancreatitis was originally developed by Huang *et al.* (2014). Mice received two hourly injections of ethanol (1.35 g kg<sup>-1</sup>, i.p.) mixed with palmitoleic acid (POA; 150 mg kg<sup>-1</sup>, i.p.) to prevent ethanol-induced peritoneal irritation, 200 µl physiological saline was injected before the ethanol/POA treatment. One hour after the first and directly before the second ethanol/POA injection, CM5480 (20 mg kg<sup>-1</sup>, i.p.) was administered. Control mice received 200 µl physiological saline (i.p.) instead of ethanol/POA. Twenty-four hours after the first ethanol/POA treatment, the mice were sacrificed under pentobarbital (85 mg kg<sup>-1</sup>, i.p.) anaesthesia.

For all experimental AP models, histological parameters were monitored to estimate the severity of induced pancreatitis. For histological scoring, pancreata were quickly removed, cleaned from fat and lymph nodes, and stored at 4°C in 4% formaldehyde. Paraffin-embedded pancreas samples were sliced in 4 µm-thick sections and stained with haematoxylin–eosin. To estimate severity of induced pancreatitis, oedema, inflammatory cell infiltration and necrosis of the samples were scored by three independent investigators blinded to the protocol (0–5 points for oedema and leukocyte infiltration, or percentage of total area for necrosis; Fanczal *et al.* 2020). Averages of the obtained scores are included in the Results.

### ***In vivo* measurement of pancreatic fluid secretion**

In all experimental AP models, pancreatic fluid was collected *in vivo* directly before sacrifice. Mice were anaesthetized with a ketamine/xylazine cocktail (respectively 125 and 12.5 mg kg<sup>-1</sup>, i.p.) and placed on a heated pad to maintain body temperature. The operation was performed as described in cases of 4% Na-TC-induced AP. Following stimulation with secretin (0.75 clinical unit kg<sup>-1</sup>, i.p.) for 30 min, the pancreatic juice was collected and the secretory rate was calculated as µl/body weight in g for 1 h.

### **Statistics**

Statistical analysis was performed with GraphPad Prism (GraphPad Software, La Jolla, CA, USA). All data are expressed as means ± SD. Both parametric (Tukey's multiple comparisons test) and non-parametric (Mann–Whitney test and Kruskal–Wallis test used for analysis of the organoid cell survival assay) tests were used based on the normality of data distribution. The specific statistical analysis is indicated in the figure legends for each experimental condition. A *P*-value below

0.05 was considered statistically significant. The first *n* number defines the number of animals and the second *n* number is the number of independent experiments (ductal fragments/organoids) analysed.

## **Results**

### **Orai1 is expressed on the apical plasma membrane of pancreatic ductal epithelia**

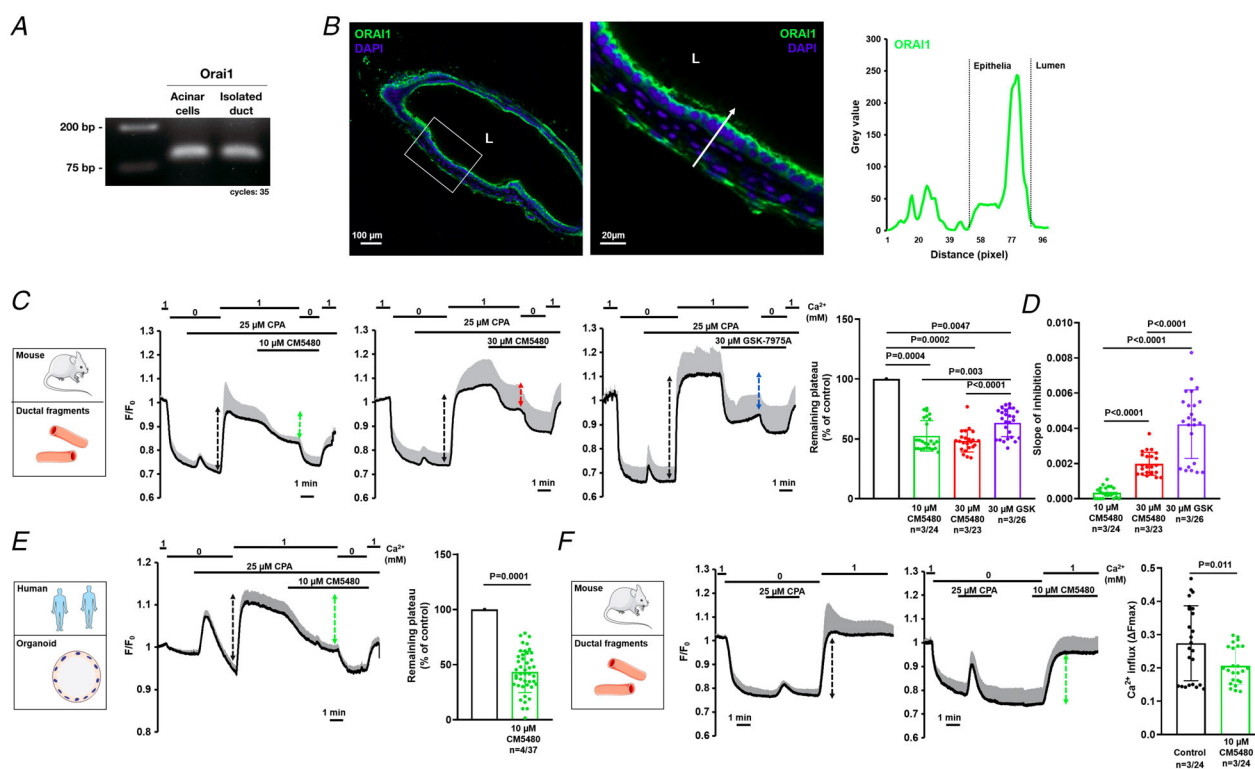
First, we analysed the expression of Orai1 in mouse primary pancreatic ductal epithelial cells. End-point PCR analysis of isolated acini and ductal fragments confirmed that Orai1 is expressed in pancreatic ductal cells (Fig. 1A). Immunofluorescent labelling of cross sections of isolated mouse pancreatic ducts revealed that Orai1 is localized dominantly on the apical PM of the pancreatic ductal epithelia (Fig. 1B). Of note, Orai1 was also detected in cells surrounding the ductal epithelia (most likely fibroblasts) and Orai1 expression on the basolateral membrane of the ductal cells cannot be excluded due to the resolution limit of the light microscopy. Next, to demonstrate Orai1 functionality in mouse pancreatic ductal cells, ER Ca<sup>2+</sup> stores were depleted with 25 µM cyclopiazonic acid (CPA) in Ca<sup>2+</sup>-free extracellular medium to activate SOCE. Under these conditions, re-addition of 1 mM extracellular Ca<sup>2+</sup> resulted in a marked extracellular Ca<sup>2+</sup> influx, which was impaired by 10 µM CM5480, a potent Orai1 inhibitor (Fig. 1C). Although the maximal inhibition did not increase when using a higher concentration of CM5480, resulting in a similar decrease of the plateau phase (45.15 ± 3.41% at 10 µM CM5480 vs. 52.38 ± 2.45% at 30 µM CM5480), inhibition was achieved significantly faster at 30 µM CM5480 (Fig. 1D). To compare the effect of CM5480 to a known Orai1 inhibitor, we applied 30 µM GSK-7975A during the same protocol. We found that although the inhibitory effect of GSK-7975A was achieved significantly faster than CM5480, the maximal inhibition was higher during CM5480 administration. Then, we applied the same protocol to human pancreatic organoids consisting of primary polarized ductal cells. In these organoids, 10 µM CM5480 remarkably decreased the extracellular Ca<sup>2+</sup> influx (56.63 ± 2.85%) indicating that Orai1 is active in the human pancreatic ducts (Fig. 1E). As the plateau phase of the Ca<sup>2+</sup> signal under the applied conditions is a mixture of Ca<sup>2+</sup> influx and efflux, which may affect the characterization of the Orai1-mediated Ca<sup>2+</sup> entry, we also applied another protocol. Similarly, in mouse pancreatic ducts, addition of CM5480 before the re-addition of extracellular Ca<sup>2+</sup> resulted in a significant decrease of the extracellular Ca<sup>2+</sup> influx (Fig. 1F). Of note, despite the inhibition of the Orai1 channels, a significant proportion of the extracellular Ca<sup>2+</sup> influx remained active in every case suggesting that other Ca<sup>2+</sup> influx channels or

transporters may contribute to the extracellular  $\text{Ca}^{2+}$  influx in ductal cells.

### The inhibition of Orai1 abolishes toxin-induced extracellular $\text{Ca}^{2+}$ influx in the pancreatic ductal epithelia

Next, we investigated the role of Orai1-mediated  $\text{Ca}^{2+}$  entry in the development of bile acids or ethanol and ethanol metabolite-induced sustained intracellular  $\text{Ca}^{2+}$  elevation. In these experiments, isolated murine pancreatic ductal fragments were challenged with 250  $\mu\text{M}$  CDC, known to induce a sustained elevation of the intracellular  $\text{Ca}^{2+}$  concentration (Venglovecz *et al.* 2008), or with a combination of 100 mM ethanol

and 200  $\mu\text{M}$  PA. Next, following reaching a stable plateau, the ductal fragments were challenged with 10  $\mu\text{M}$  CM5480. Based on the  $\Delta F$  value of the plateau, CM5480-mediated inhibition of Orai1 significantly decreased the extracellular CDC-induced  $\text{Ca}^{2+}$  influx. However, as the plateau phase of the evoked  $\text{Ca}^{2+}$  signal was not clearly separated from the peak in cases of ethanol/PA, we decided to apply CM5480 simultaneously with the EtOH+PA treatment. Similar to CDC, CM5480-mediated inhibition of Orai1 significantly impaired the effect of ethanol/PA-induced  $\text{Ca}^{2+}$  influx and also reduced the area under the curve (Fig. 2A–C). These results suggest the potential of CM5480 or Orai1 inhibition to prevent  $\text{Ca}^{2+}$ -overload-mediated functional and morphological damage of ductal cells associated with biliary- or ethanol-induced AP.



### Inhibition of Orai1 prevents bile acid- and ethanol-induced decrease of $\text{HCO}_3^-$ secretion and CFTR function in pancreatic ductal epithelia

$\text{HCO}_3^-$  secretion – the primary function of pancreatic ductal epithelia – is significantly impaired by bile acid- and ethanol-mediated sustained  $\text{Ca}^{2+}$  elevation and mitochondrial damage (Maléth *et al.* 2015; Molnár *et al.* 2020). To assess the potential protective effect of Orai1 inhibition on ductal  $\text{HCO}_3^-$  secretion, we treated isolated murine ductal fragments with CDC or ethanol/PA in the presence or absence of CM5480 and compared  $\text{HCO}_3^-$  efflux across the apical membrane (Maléth *et al.* 2015). In these experiments, exposure of the ductal cells to 20 mM  $\text{NH}_4\text{Cl}$  in  $\text{HCO}_3^-/\text{CO}_2$ -buffered solution triggered a rapid alkalization caused by the passive  $\text{NH}_3$  uptake of the cells, which was followed by a slow recovery of the alkaline pH, due to the  $\text{SLC26 Cl}^-/\text{HCO}_3^-$  exchanger, and CFTR-mediated  $\text{HCO}_3^-$  (Molnár *et al.*

2020) efflux (i.e. secretion) from the ductal epithelia to resting  $\text{pH}_i$  (Fig. 3A). Subsequent removal of  $\text{NH}_4\text{Cl}$  rapidly decreased  $\text{pH}_i$  below the resting value, which was later restored due to basolateral  $\text{NHE1}$  and  $\text{NBCe1}$  channel activity. To calculate the base flux values ( $J_B$ ) of  $\text{HCO}_3^-$  extrusion (calculated as  $\Delta\text{pH}/\Delta t$ ; Molnár *et al.* 2020), the initial recovery rates were measured over the first 30 s. By using this approach, we found that CM5480 significantly improved the apical  $\text{HCO}_3^-$  efflux in the CDC- or ethanol/PA-treated isolated ducts (Fig. 3C). Next, we used the intracellular  $\text{Cl}^-$  ( $[\text{Cl}^-]_i$ )-sensitive fluorescent indicator MQAE to follow CFTR-driven  $\text{Cl}^-$  extrusion in intact pancreatic ductal fragments (Fig. 3B). Considering that MQAE-mediated fluorescence inversely correlates with  $[\text{Cl}^-]_i$ , an increased MQAE signal reports  $\text{Cl}^-$  efflux. Removal of extracellular  $\text{Cl}^-$  from the  $\text{HCO}_3^-/\text{CO}_2$ -buffered solution resulted in a  $[\text{Cl}^-]_i$  decrease, most likely due to CFTR-mediated  $\text{Cl}^-$  efflux from the cytosol (Molnár *et al.* 2020). While treatment of ductal cells with 250  $\mu\text{M}$  CDC or 100 mM

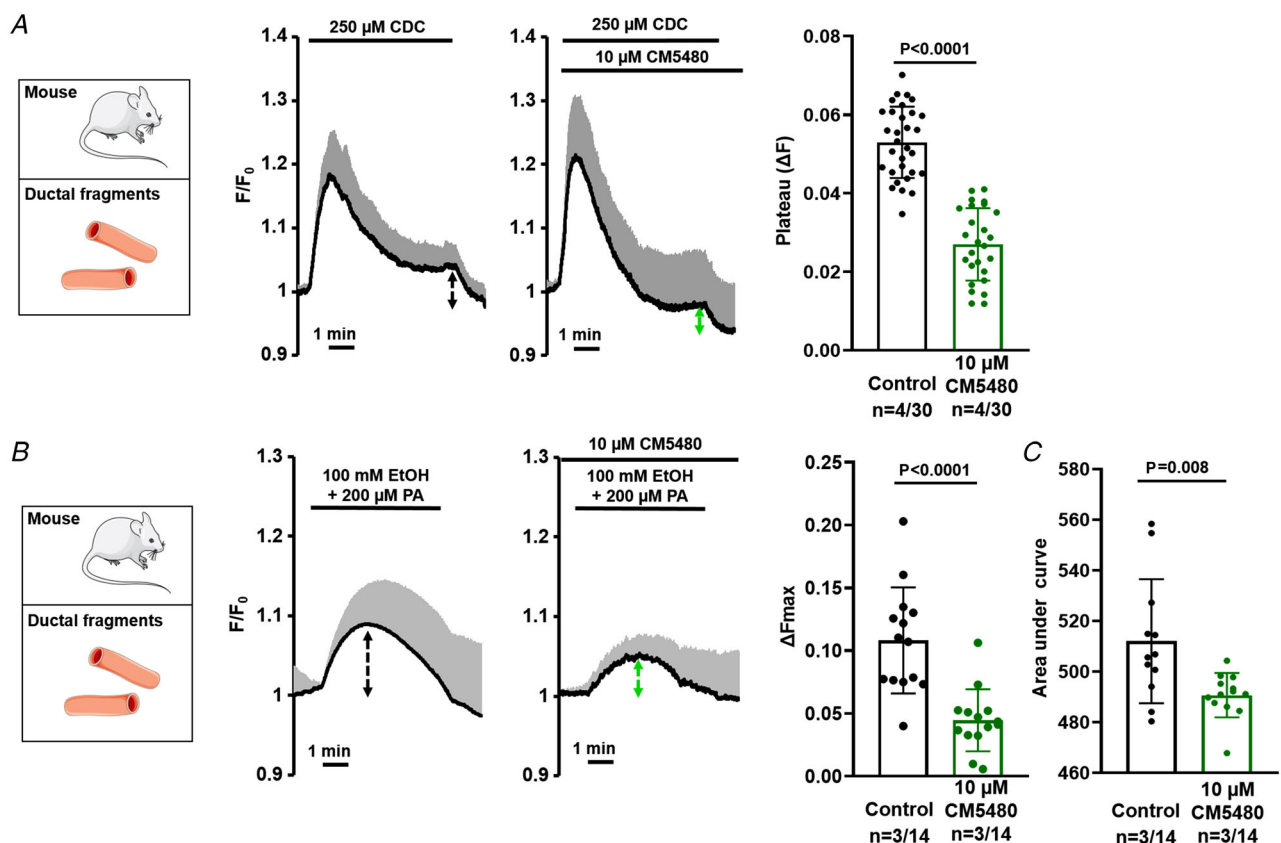


**Figure 2. Pharmacological inhibition of Orai1 leads to reduced extracellular  $\text{Ca}^{2+}$  influx induced by bile acid or ethanol and fatty acid in pancreatic ductal epithelia**

Isolated mouse pancreatic ductal fragments were challenged with 250  $\mu\text{M}$  CDC or with a combination of 100 mM ethanol and 200  $\mu\text{M}$  PA in standard HEPES-buffered solution. A, average traces and the bar charts demonstrate that the inhibition of Orai1 by 10  $\mu\text{M}$  CM5480 significantly decreased the plateau phase of the CDC-induced intracellular  $\text{Ca}^{2+}$  signal. B and C, Orai1 inhibition also reduced the intracellular  $\text{Ca}^{2+}$  elevation and value of area under curve triggered by the combination of 100 mM ethanol and 200  $\mu\text{M}$  PA. Statistical analysis was performed with the Mann–Whitney test.

ethanol/200  $\mu\text{M}$  PA resulted in a significant drop of CFTR activity, this was significantly improved by co-administration of 10  $\mu\text{M}$  CM5480 (Fig. 3B and D). These results suggest that CM5480 treatment has the potential to prevent the AP-induced inhibition of the pancreatic ductal  $\text{HCO}_3^-$  secretion and partially restored CFTR activity.

### Inhibition of Orai1 prevents bile acid- and ethanol-induced cell death in pancreatic ductal epithelia

Considering that bile acid- and ethanol metabolite-induced sustained intracellular  $\text{Ca}^{2+}$  elevation is known to trigger cell death (Voronina *et al.* 2002;

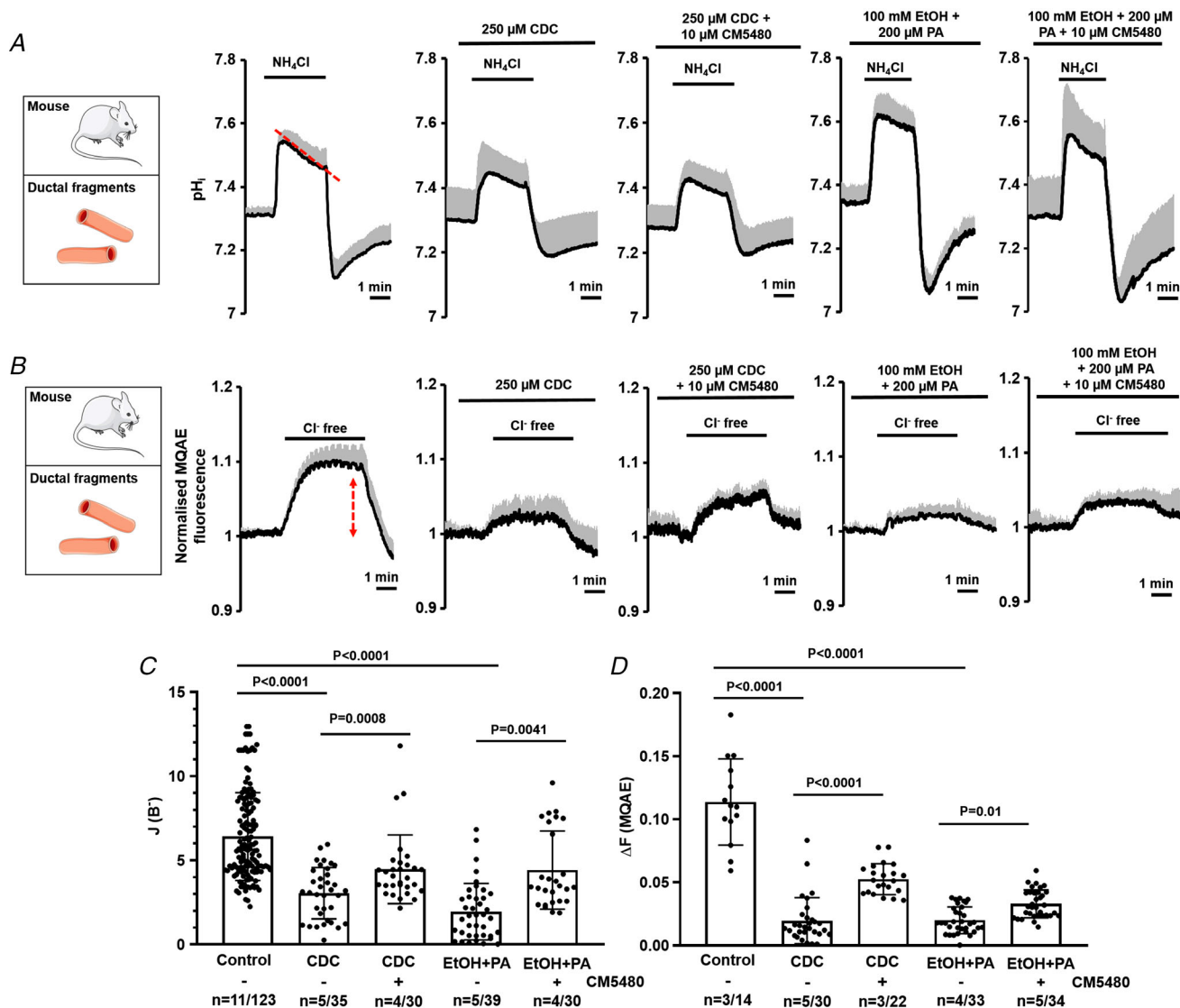


**Figure 3. The inhibition of Orai1 prevents bile acid- and ethanol-induced decrease of apical  $\text{HCO}_3^-$  secretion and CFTR function in pancreatic ductal epithelia**

A, mouse pancreatic ducts were perfused with 250  $\mu\text{M}$  CDC or 100 mM ethanol and 200  $\mu\text{M}$  PA in  $\text{HCO}_3^-/\text{CO}_2$ -buffered extracellular solution and intracellular alkalinization was achieved by 20 mM  $\text{NH}_4\text{Cl}$  administration in the absence or presence of Orai1 inhibitor CM5480. Both pathogenic conditions significantly reduced the base flux, which was offset using the Orai1 inhibitor. B, average traces of intracellular  $\text{Cl}^-$  levels reflecting CFTR activity in mouse isolated ductal fragment using  $\text{Cl}^-$ -sensitive fluorescent dye (MQAE). Removal of extracellular  $\text{Cl}^-$  induced a decrease in intracellular  $\text{Cl}^-$  levels (reflected by an increase in fluorescence intensity) due to CFTR activity.  $\text{Cl}^-$  removal from the extracellular solutions in the presence of 250  $\mu\text{M}$  CDC or 100 mM ethanol and 200  $\mu\text{M}$  PA inhibited CFTR activity, which was improved by CM5480. C and D, bar charts of the calculated base fluxes of  $\text{HCO}_3^-$  (C) and  $\text{Cl}^-$  efflux (D). CM5480 significantly increased both parameters in the presence of CDC, ethanol+PA. Statistical analysis was performed with Tukey's multiple comparisons test.

Criddle *et al.* 2006), we next sought to characterize the effects of Orai1 inhibition on pancreatic ductal cell survival. For this, we used mouse pancreatic ductal organoids as they are more suitable for reaching single cell resolution with a confocal microscope allowing reliable counting of labelled cells. Also, as no other cell type surrounds the epithelial monolayer in these organoids,

we are confident we were only quantifying epithelial cell death (Fig. 4A). In the untreated control samples, minimal cell damage was observed (percentage of viable cells:  $92.2 \pm 3.4$ ). Incubation of pancreatic ductal organoids with CDC or EtOH+PA for 30 min remarkably decreased the number of viable cells and significantly increased necrotic cell death (percentage of viable cells:  $49.4 \pm 5.3$

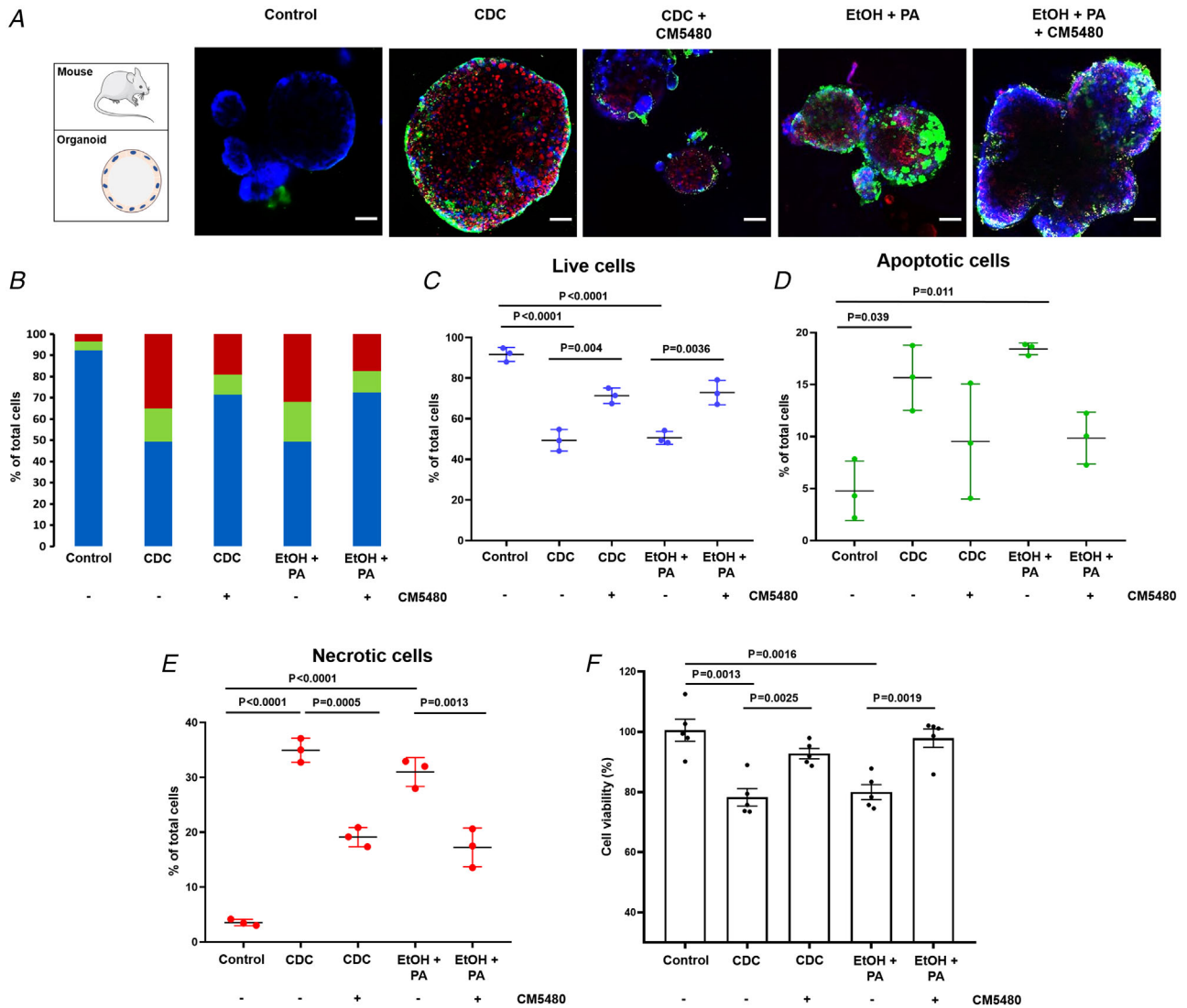


**Figure 4. Inhibition of Orai1 prevents bile acid- and ethanol-induced cell death in the pancreatic ductal epithelia**  
 A, representative confocal z-stack images of mouse pancreatic ductal organoids under different treatment conditions (blue: live cells labelled with CytoCalcein 450, green: necrotic cells labelled with Nuclear Green, and red: apoptotic cells labelled with Apopxin Deep Red). Scale bar: 50  $\mu$ m. B, bar chart representing the percentage of live, apoptotic and necrotic cells in the organoids after incubation with 250  $\mu$ M CDC or 100 mM EtOH and 200  $\mu$ M PA in the presence and absence of 10  $\mu$ M CM5480 for 30 min at 37°C. C–E, treatment of the organoids with CDC or with ethanol+PA markedly decreased the number of viable cells (C), whereas the number of apoptotic (D) and necrotic (E) cells was significantly increased; 10  $\mu$ M CM5480 markedly decreased the rate of apoptotic and significantly reduced necrotic cells and in parallel increased the number of detectable live cells. F, bar charts summarizing the cell viability as measured by the ATP-dependent bioluminescence using CellTiter-Glo 3D cell viability assay. Treatment conditions were the same as above described. CM5480 treatment significantly increased the cell viability compared to CDC or EtOH+PA treated groups. Statistical analysis was performed with the Kruskal–Wallis test.

and  $50.6 \pm 3.2$ , respectively) (Fig. 4B–E). Similarly, the apoptosis rate significantly increased upon CDC or EtOH+PA administration. Although CM5480-mediated Orai1 inhibition decreased the percentage of apoptotic cells to some extent, this improvement failed to reach statistical significance (Fig. 4D). However, both in bile acid- and alcohol-treated organoids, CM5480-mediated Orai1 inhibition significantly decreased the percentage of necrotic cells (Fig. 4E). Importantly, inhibition of Orai1 resulted in about 45% less pancreatic ductal cell death, suggesting an important role of Orai1-mediated extracellular  $\text{Ca}^{2+}$  influx in biliary- and alcoholic AP-mediated ductal cell death. The availability of ATP is crucial to determination of cell fate during stress. To provide an insight into the changes of the intracellular ATP in the different conditions, we measured the cell viability using a CellTiter-Glo 3D cell viability assay (Fig. 4F). Our results showed that incubation of pancreatic ductal organoids with CDC or EtOH+PA for 30 min caused significant reduction of the ATP-dependent bioluminescence, which was almost completely restored by CM5480.

### Bile acid- and alcohol-induced Orai1-mediated extracellular $\text{Ca}^{2+}$ entry depends on the activation of Stim1

Exposure of ductal cells to bile acids and ethanol releases  $\text{Ca}^{2+}$  from intracellular stores most prominently from the ER (Mal  th *et al.* 2011, 2015), which induces a conformational change of Stim1 triggering Orai1-mediated  $\text{Ca}^{2+}$  influx. To assess the involvement of Stim1 in bile acid- and alcohol-induced ductal cell functional damage, we treated isolated ducts with specific siRNA to knock down Stim1 expression. Treatment of pancreatic ductal cells with siStim1 did not alter CFTR-mediated  $\text{HCO}_3^-$  or  $\text{Cl}^-$  secretion (Fig. 5A and B). Whereas CDC or ethanol/PA significantly impaired  $\text{HCO}_3^-$  secretion or CFTR activity in siGLO-Green-treated pancreatic ductal cells, this was prevented in siStim1-treated cells (Fig. 5C). These results suggest that bile acids and ethanol induce Orai1-mediated  $\text{Ca}^{2+}$  influx in a Stim1-dependent manner.

### The effect of CM5480 on experimental acute pancreatitis

Based on our obtained results, we wanted to confirm the protective effect of Orai1 inhibition on ductal secretion *in vivo*. To analyse the potential of CM5480 to reduce the severity of experimental AP, we used three independent experimental models. In the first experimental model, mice received seven hourly injections of cerulein ( $50 \mu\text{g kg}^{-1}$ , i.p.) to induce pancreatitis (Fig. 6A). Similar to

previous independent reports (Wen *et al.* 2015; Waldron *et al.* 2019), inhibition of Orai1 by CM5480 ( $20 \text{ mg kg}^{-1}$ , i.p.) – administered after the second cerulein injection – significantly reduced the histological inflammatory parameters (Fig. 6A).

Next, AP was induced by intraductal infusion of 4% Na-TC. In these experiments, administration of CM5480 ( $20 \text{ mg kg}^{-1}$ , i.p.) 1 h after the Na-TC infusion improved the oedema and leukocyte infiltration, although tissue necrosis was only moderately decreased (Fig. 6B). Despite the lack of a significant decrease in necrosis by CM5480, this experimental protocol allowed us to study the changes of *in vivo* fluid secretion (see below). Likely, a further decrease of necrosis might have been obtained in cases of repetitive CM5480-administration.

Finally, in the third experimental AP model, mice received a mixture of ethanol and POA to mimic alcohol-induced AP (Fig. 6C). In this model, administration of CM5480 ( $20 \text{ mg kg}^{-1}$ , i.p.) directly before the second ethanol/POA injection significantly improved AP-mediated oedema and necrosis but only moderately decreased leukocyte infiltration.

### Inhibition of Orai1 preserves pancreatic ductal secretion *in vivo* during acute pancreatitis

Finally, we wanted to provide evidence that inhibition of Orai1 prevents AP-mediated impairment of pancreatic ductal function *in vivo* as well. For this, we chose to use the same model systems as described above, as they successfully reproduced previously reported data, to analyse AP-mediated changes of fluid secretion *in vivo*. Upon establishment of experimental AP, secretin-induced fluid secretion was measured *in vivo* in anaesthetized mice. While *in vivo* fluid secretion was significantly impaired in all three AP groups (i.e. cerulein-, Na-TC- and ethanol/POA-treated animals), it was most pronounced in the cerulein-treated group (Fig. 7A), although still more than 60% impaired in the two other AP groups. Importantly, whereas CM5480 treatment alone did not affect secretin-stimulated pancreatic secretion, it preserved the *in vivo* fluid secretion in the AP mice. In fact, in both cerulein- and ethanol/POA-treated animals, CM5480 significantly improved *in vivo* fluid secretion to levels comparable to the untreated – healthy – control group (Fig. 7A and C). Moreover, in the Na-TC-treated group, CM5480 resulted in an almost twofold increased fluid secretion compared to the Na-TC group; however, the difference failed to reach statistical significance (Fig. 7B). To further confirm these results, we isolated pancreatic ductal fragments from cerulein-induced AP mice and measured *in vitro*  $\text{HCO}_3^-$  secretion (Fig. 7D). As expected, whereas cerulein significantly decreased  $\text{HCO}_3^-$  secretion in the ductal fragments,

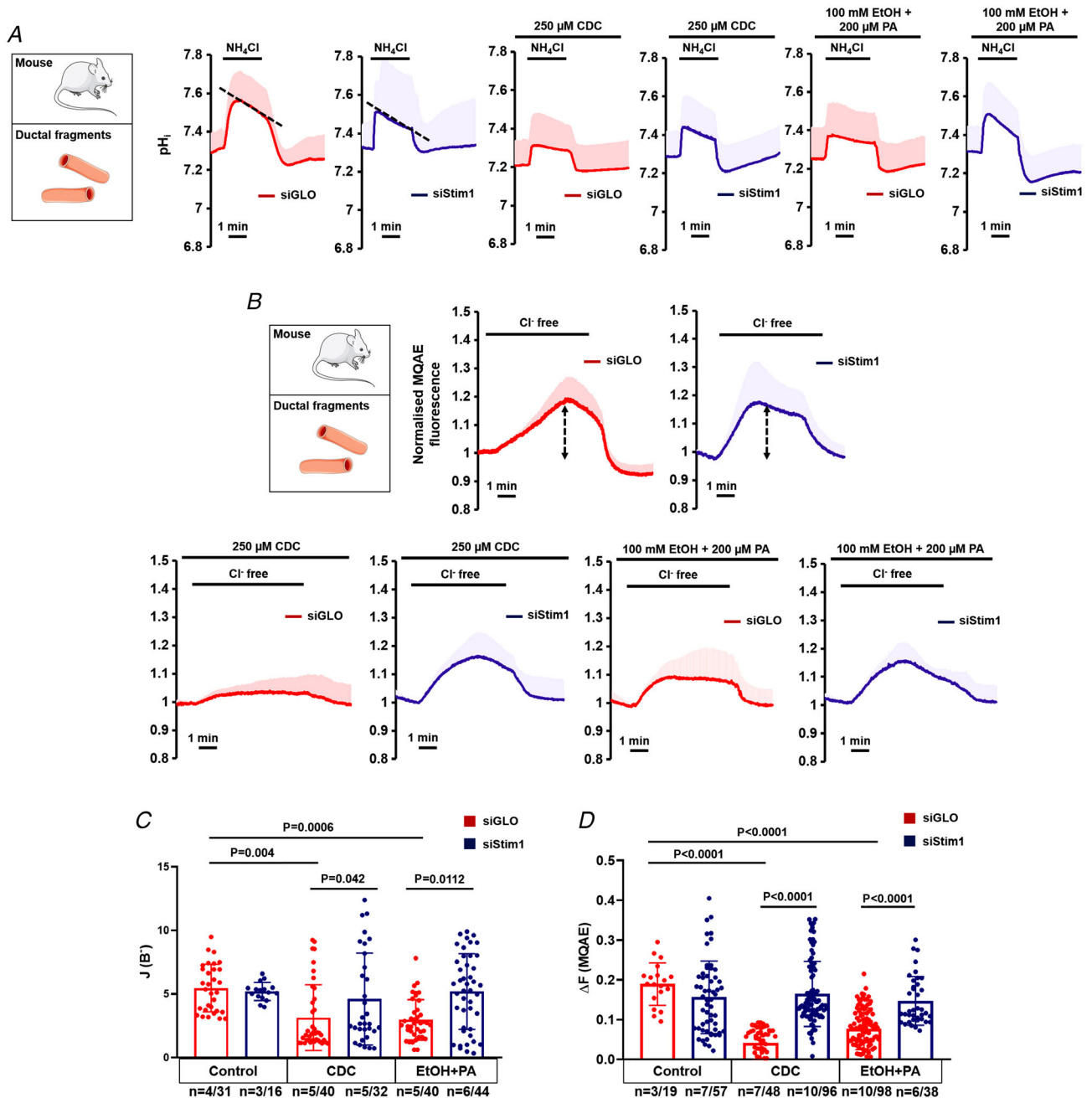


**Figure 5.** siStim1 treatment prevents bile acid- and ethanol-induced decrease of apical  $\text{HCO}_3^-$  secretion and CFTR function in pancreatic ductal epithelia

Average traces and bar charts demonstrate the effects of 250  $\mu\text{M}$  CDC or 100 mM ethanol and 200  $\mu\text{M}$  PA on control (red traces) and siStim1-treated (blue traces) pancreatic ductal fragments. **A**, pancreatic ducts were challenged with 20 mM  $\text{NH}_4\text{Cl}$  in  $\text{HCO}_3^-/\text{CO}_2$ -buffered extracellular solution and the apical  $\text{Cl}^-/\text{HCO}_3^-$  exchange activity was determined. **B**, extracellular  $\text{Cl}^-$  was removed to measure CFTR activity in control and treated ductal fragments. **C** and **D**, bar charts of the calculated base fluxes of  $\text{HCO}_3^-$  or maximal fluorescent intensity changes of MQAE show that administration of CDC or ethanol+PA significantly impaired pancreatic ductal  $\text{HCO}_3^-$  secretion and CFTR-mediated  $\text{Cl}^-$  secretion in the siGLO-Green-treated control ducts. siStim1 treatment prevented the inhibition of these parameters. Statistical analysis was performed with Tukey's multiple comparisons test.

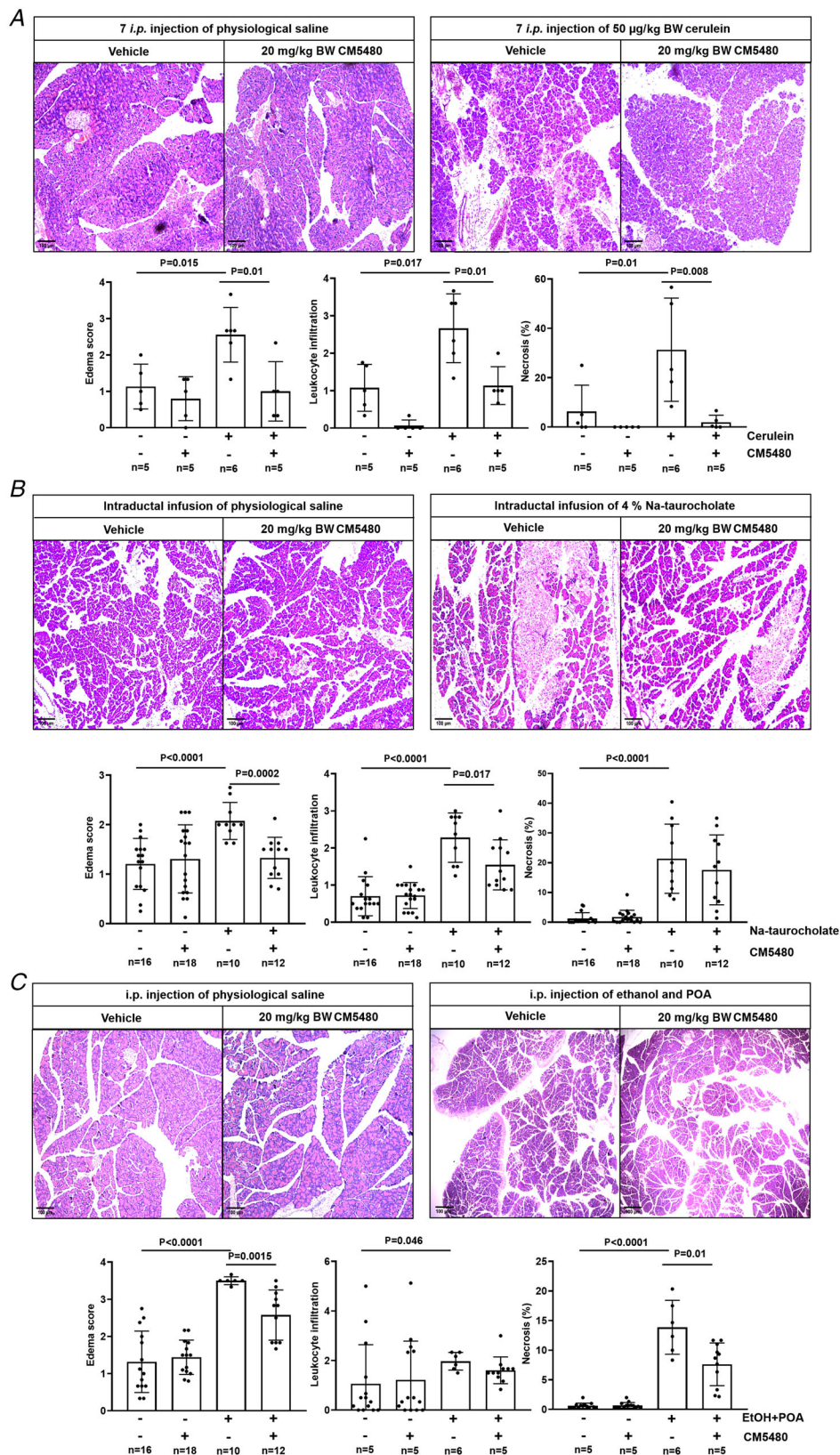


**Figure 6. Orai1 inhibition by CM5480 reduces the severity of acute pancreatitis**  
 A, representative images of pancreatic histology in cerulein-induced pancreatitis. Mice were given 7 hourly i.p. injections of either physiological saline (PS, control group) or 50 µg kg<sup>-1</sup> cerulein. CM5480 or vehicle was

administered 1 h after the first injection of cerulein or PS. Cerulein administration caused extensive pancreatic damage, which was significantly reduced by 20 mg (kg BW)<sup>-1</sup> CM5480 treatment. *B*, representative images of pancreatic histology in sodium taurocholate (Na-TC)-induced pancreatitis. Pancreatitis was induced by intraductal infusion of 4% Na-TC. CM5480 or vehicle was administered 1 h after the Na-TC or PS infusion. Four percent Na-TC induced necrotizing pancreatitis in mice accompanied by elevated histological parameters. Orai1 inhibition by CM5480 significantly reduced the extent of oedema and leukocyte infiltration; however, there was no significant difference in the extent of necrosis. *C*, representative images of pancreatic histology in ethanol+palmitoleic acid (POA)-induced pancreatitis. Mice were given 2 hourly i.p. injections of either PS or 1.75 g kg<sup>-1</sup> ethanol and 750 mg kg<sup>-1</sup> POA. CM5480 or vehicle was administered 1 h after the first injection. Orai1 inhibition significantly improved the oedema and necrosis induced by ethanol+POA, whereas no significant difference was observed in leukocyte infiltration. Scale bar: 100  $\mu$ m. Statistical analysis was performed with Tukey's multiple comparisons test.

this secretory activity was preserved in ductal fragments derived of cerulein-induced AP mice receiving CM5480. Importantly, these results confirmed that inhibition of Orai1 preserves the ductal ion and fluid secretion both *in vitro* and *in vivo* in different forms of AP.

## Discussion

Regardless of its aetiology, sustained elevation of intracellular Ca<sup>2+</sup> is a hallmark of the development of AP-mediated cellular injury (Mal  th & Hegyi, 2016;

Pallagi *et al.* 2020). Although selective Orai1 inhibitors limiting the excessive extracellular Ca<sup>2+</sup> influx prevented acinar cell damage and decreased the severity of AP in multiple animal models (Wen *et al.* 2015; Waldron *et al.* 2019), precisely how Orai1 inhibition affects the pancreatic ductal cell functions is currently unknown. In this study, we first demonstrated that Orai1 resides in the apical PM of the pancreatic ductal cells where it mediates extracellular Ca<sup>2+</sup> influx upon ER Ca<sup>2+</sup> store depletion. Next, we provided evidence that bile acid- and ethanol-mediated SOCE activation contribute

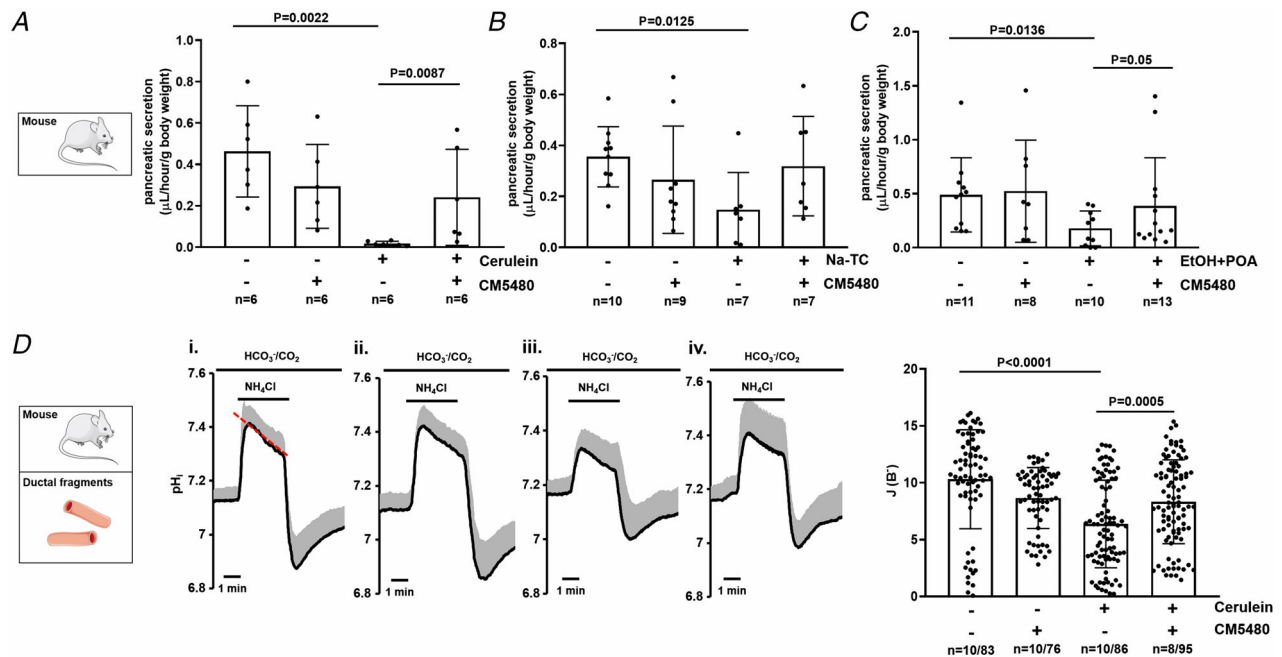


**Figure 7. Orai1 inhibition by CM5480 prevents pancreatic ductal secretion during acute pancreatitis**

Acute pancreatitis (AP) was induced in mice as described above. Pancreatic juice was collected for 30 min *in vivo* under secretin-stimulated (0.75 CU kg<sup>-1</sup> i.p.) conditions from anaesthetized mice after induction of AP. *A*, summary bar charts show that cerulein administration significantly reduced the volume of pancreatic juice, which was preserved by CM5480 treatment. *B*, CM5480 administration increased the reduced *in vivo* fluid secretion caused by Na-taurocholate, but the difference was not significant. *C*, the volume of pancreatic juice was significantly lower after ethanol+POA treatment; however, Orai1 inhibition significantly improved it. *D*, average traces and bar charts demonstrate the *in vitro* HCO<sub>3</sub><sup>-</sup> secretion of pancreatic ductal fragments isolated from mouse pancreas after the induction of AP with cerulein. Pancreatic ducts were perfused with HCO<sub>3</sub><sup>-</sup>/CO<sub>2</sub>-buffered extracellular solution and intracellular alkalization was achieved by 20 mM NH<sub>4</sub>Cl administration. Comparison of recovery from alkalosis shows that ductal HCO<sub>3</sub><sup>-</sup> secretion was significantly reduced in the cerulein-treated group, and was restored by CM5480 treatment. Statistical analysis was performed with Tukey's multiple comparisons test. [Colour figure can be viewed at [wileyonlinelibrary.com](http://wileyonlinelibrary.com)]

to sustained intracellular  $\text{Ca}^{2+}$  elevations leading to damaged ductal secretion and cell death. Finally, prevention of intracellular  $\text{Ca}^{2+}$  overload with selective Orai1 inhibitors preserved pancreatic ductal ion and fluid secretion and maintained exocrine pancreatic secretion during AP.

Expression of Orai1 in exocrine pancreatic acinar cells was previously described by two independent groups. Lur *et al.* (2009) demonstrated Stim1 translocation and Orai1 activation in the lateral and basal plasma membrane, whereas Hong *et al.* (2011) reported a more pronounced Orai1 expression in the apical membrane. In our experiments, Orai1 expression was observed on the apical membrane of ductal cells, but not on the basolateral membrane. Although the significance of this polarized expression pattern is currently unknown, it may be of importance in reuptake of intraluminal  $\text{Ca}^{2+}$  secreted by the acinar cells during digestive enzyme secretion. Interestingly, CM5480-mediated functional inhibition of Orai1 did not completely abolish the ER store depletion-induced extracellular  $\text{Ca}^{2+}$  influx. In fact, in the current study, we achieved a maximal inhibition of around 50% – in cases of both 10 and 30  $\mu\text{M}$  CM5480 – suggesting that additional PM-residing  $\text{Ca}^{2+}$  channels or transporters contribute to SOCE in ductal cells. When compared to a known Orai1 inhibitor – GSK-7975A – CM5480 achieved significantly higher inhibition of the extracellular  $\text{Ca}^{2+}$  influx, but GSK-7975A reached the maximal inhibitory effect more rapidly. Interestingly, genetic deletion of the TRPC3  $\text{Ca}^{2+}$  channel resulted in a 50% reduction of receptor-stimulated SOCE in pancreatic acinar cells and prevented bile acids- and ethanol metabolite-induced sustained  $\text{Ca}^{2+}$  elevation and intracellular trypsin activation. These beneficial effects ultimately resulted in reduced cerulein-induced AP severity *in vivo* (Kim *et al.* 2009). Similar results were achieved with the specific TRPC3 inhibitor Pyr3 (Kim *et al.* 2011). However, the contribution of TRPC3 to SOCE in pancreatic ductal cells is currently unknown. On the other hand, the accessibility of the apical membrane in these *ex vivo* models may be limited as the ductal fragments are sealed and the epithelial cells in the organoids form a polarized and closed monolayer, which can limit the diffusion of the drugs to the apical membrane proteins.

To achieve strict control and tune the activity of each other,  $\text{Ca}^{2+}$  and cAMP/protein kinase A signalling, a well-known key regulator of CFTR activity and  $\text{HCO}_3^-$  secretion, interact at multiple levels to facilitate maximal response (Ahuja *et al.* 2014). On the other hand, the most common biologically active molecules inducing AP, including bile acids, non-oxidative ethanol metabolites and trypsin, induce toxic, sustained intracellular  $\text{Ca}^{2+}$  elevation in the exocrine pancreas (Voronina *et al.* 2002; Criddle *et al.* 2006). Previous data indicated that the

non-conjugated bile acid CDC dose-dependently impairs pancreatic  $\text{HCO}_3^-$  secretion (Venglovecz *et al.* 2008) via sustained  $\text{Ca}^{2+}$  elevation and subsequent mitochondrial damage in pancreatic ductal (Mal  th *et al.* 2011) cells and isolated pancreatic acinar cells (Gerasimenko *et al.* 2006).

Considering the detrimental effect of heavy ethanol consumption in combination with non-oxidative ethanol metabolites (such FAEE) on acinar and ductal cells (Petersen *et al.* 2009; Mal  th & Hegyi, 2014), our group previously demonstrated that EtOH+POA impaired the activity of the apical SLC26  $\text{Cl}^-/\text{HCO}_3^-$  exchanger and CFTR  $\text{Cl}^-$  channel together with decreased  $\text{HCO}_3^-$  secretion in ductal cells (Mal  th *et al.* 2015). Mechanistically, ethanol and POA induced a sustained  $\text{Ca}^{2+}$  elevation through  $\text{IP}_3$ - and ryanodine receptor-mediated  $\text{Ca}^{2+}$  release from the ER combined with extracellular  $\text{Ca}^{2+}$  influx, a mechanism which was also described in pancreatic acinar cells (Criddle *et al.* 2004, 2006, 2007). The involvement of Orai1 in the development of AP was first highlighted by Gerasimenko *et al.* (2013) demonstrating that Orai1 inhibition decreased acinar cell necrosis *in vitro*. In fact, selective GSK-7975A-mediated inhibition of Orai1 inhibited SOCE in a concentration-dependent manner and reduced the sustained  $\text{Ca}^{2+}$  elevation, trypsin activation and acinar necrosis upon FAEE exposure. Others found that GSK-7975A and CM\_128 markedly impaired bile acid-induced extracellular  $\text{Ca}^{2+}$  influx and sustained  $\text{Ca}^{2+}$  overload in pancreatic acinar cells and significantly decreased pancreatic oedema, inflammation and necrosis in experimental models of AP (Wen *et al.* 2015). Waldron *et al.* (2019) showed that inhibition of SOCE by CM4620 prevented trypsinogen activation, acinar cell death, nuclear factor- $\kappa\text{B}$  and nuclear factor of activated T cells (NFAT) activation, and inflammatory responses in multiple *in vitro* and *in vivo* models. Other reports described cerulein-mediated interaction between Stim1 and Orai1, subsequent activation of SOCE, and calcineurin-mediated activation of NFAT and transcription factor EB promoting transcription of chemokine and autophagy-associated genes (Zhu *et al.* 2018). In our study, inhibition of Orai1 by CM5480 in pancreatic ductal cells significantly decreased the bile acid- and ethanol/PA-mediated extracellular  $\text{Ca}^{2+}$  influx in pancreatic ductal fragments and organoids. The CM5480-mediated inhibition of Orai1 was sufficient to significantly improve the *in vitro*  $\text{HCO}_3^-$  secretion and CFTR activity in pancreatic ductal cells. Moreover, CM5480 preserved the intracellular ATP production, significantly improved the overall ductal cell survival and remarkably prevented CDC- and ethanol/PA-induced cell necrosis. Interestingly, Orai1 inhibition prevented the decrease of ATP production, but it did not completely abolish necrotic cell death. Notably, our previous work showed that bile acids can damage the mitochondria

independently of  $\text{Ca}^{2+}$  overload, as BAPTA was not able to prevent the mitochondrial damage (Mal  th *et al.* 2011). As specific siRNA knockdown of the ER  $\text{Ca}^{2+}$  sensor protein Stim1 reproduced the effect of selective pharmacological Orai1 inhibition, CDC- and ethanol/PA-induced activation of Orai1 seems to be Stim1 dependent.

The importance of pancreatic ductal fluid and  $\text{HCO}_3^-$  secretion in the physiological function of the exocrine pancreas is supported by several independent studies. Dimagno *et al.* (2005) demonstrated that CFTR knockout mice in which the exocrine pancreatic secretion was impaired develop more severe cerulein-induced AP, which is accompanied by increased pancreatic oedema, neutrophil infiltration and expression of inflammatory mediators. In addition, our group showed that genetic deletion of  $\text{Na}^+/\text{H}^+$  exchanger regulatory factor-1 (NHERF-1), a scaffolding protein that anchors CFTR to the apical PM, reduces pancreatic fluid and  $\text{HCO}_3^-$  secretion in mice (Pallagi *et al.* 2014). Compared to wild type littermates, NHERF-1 knockout mice developed more severe experimental AP upon cerulein hyperstimulation or bile acid infusion to the main pancreatic duct. In addition, the alcohol-induced impairment of CFTR function and expression resulted in increased severity of experimental AP. In the current study, we confirmed previous reports by indicating that *in vivo* CM5480-mediated inhibition of Orai1 in mice markedly decreases the severity of AP in three different model systems with independent pathogenic triggers. Importantly, in all three AP models, we demonstrated improved secretin-stimulated *in vivo* pancreatic fluid secretion in CM5480-treated animals. Notably, at the tested dose, CM5480 had no effects on the secretin-stimulated *in vivo* pancreatic fluid secretion itself in the control groups. Based on these and on our *in vitro* results we can conclude that bile acids and ethanol directly damage ductal cell functions, which can be restored by Orai1 inhibition. As injury of both acinar and ductal cells can affect each other's functions (Hegy   *et al.* 2011), the inhibition of Orai1 may have synergistic effects, which can improve the outcome of AP.

Restoration of pancreatic fluid secretion could have a significant beneficial impact on the disease outcome. In a healthy pancreas, the digestive enzymes produced by the acini are washed out by  $\text{HCO}_3^-$ -rich fluid into the duodenum where it neutralizes the local pH. Previously, our group demonstrated pH-dependent autoactivation of trypsinogen together with elevated trypsinogen activity in acidic environment indicating the primordial role of  $\text{HCO}_3^-$  to prevent early autoactivation of trypsinogen (Pallagi *et al.* 2011). In addition, Zeng *et al.* (2017) reported that pharmacological correction of CFTR expression and activity rescues pancreatic acinar cell function and reduces autoimmune pancreatitis-induced

inflammation, further highlighting the importance of proper ductal function in the disease outcome. Recently, the role of Saraf (Jha *et al.* 2013), an Orai1 channel regulator protein, was reported in AP (Son *et al.* 2019). In contrast to constant expression levels of Stim1 and Orai1, expression levels of Saraf decreased during AP in both mice and human. In addition, whereas Saraf knockout mice developed more severe AP accompanied by increased  $\text{Ca}^{2+}$  influx in acinar cells, its overexpression reduced acinar  $\text{Ca}^{2+}$  influx and decreased AP severity.

Very recently, a phase 2, open-label, dose-response clinical study by CalciMedica evaluated the safety of Auxora in patients with AP, SIRS and hypoxaemia (Bruen *et al.* 2021). In this clinical study, the patients received low- or high-dose Auxora plus standard of care (SOC). Overall, no differences in the number of serious adverse events with Auxora compared to SOC alone were reported. Of patients with moderate AP receiving low-dose Auxora, 36.5% improved to mild AP. Very interestingly, patients receiving Auxora better tolerated solid foods, had less persistent SIRS, and had a reduced hospitalization rate compared to SOC. It is tempting to speculate that the increased tolerance towards solid food might be explained by improved exocrine pancreatic secretion as observed in our current study. Based on these results, further clinical studies are needed to clarify the utility of Orai1 inhibition in AP patients.

Taken together, we report that inhibition of Orai1 protects pancreatic ductal cells from sustained intracellular  $\text{Ca}^{2+}$  overload triggered by bile acids and ethanol in combination with non-oxidative ethanol metabolites. Importantly, this protection seems to be sufficient to maintain crucial ductal functions such as fluid and  $\text{HCO}_3^-$  secretion both *in vitro* and *in vivo* during AP. Considering that Auxora is currently in phase 2b clinical trials to treat severe AP, our current results can further contribute to the development of specific pharmacological treatments for AP.

## References

- Ahuja M, Jha A, Mal  th J, Park S & Muallem S (2014). cAMP and  $\text{Ca}^{2+}$  signaling in secretory epithelia: crosstalk and synergism. *Cell Calcium* **55**, 385–393.
- Boj SF, Hwang CI, Baker LA, Chio II, Engle DD, Corbo V, Jager M, Ponz-Sarvisse M, Tiriac H, Spector MS, Gracianin A, Oni T, Yu KH, van Boxtel R, Huch M, Rivera KD, Wilson JP, Feigin ME,   hlund D, Handly-Santana A, Ardito-Abraham CM, Ludwig M, Elyada E, Alagesan B, Biffi G, Yordanov GN, Delcuze B, Creighton B, Wright K, Park Y, Morsink FH, Molenaar IQ, Borel Rinkes IH, Cuppen E, Hao Y, Jin Y, Nijman IJ, Iacobuzio-Donahue C, Leach SD, Pappin DJ, Hammell M, Klimstra DS, Basturk O, Hruban RH, Offerhaus GJ, Vries RG, Clevers H & Tuveson DA (2015). Organoid models of human and mouse ductal pancreatic cancer. *Cell* **160**, 324–338.

- Breunig M, Merkle J, Wagner M, Melzer MK, Barth TFE, Engleitner T, Krumm J, Wiedenmann S, Cohrs CM, Perkhofer L, Jain G, Krüger J, Hermann PC, Schmid M, Madácsy T, Á V, Griger J, Azoitei N, Müller M, Wessely O, Robey PG, Heller S, Dantes Z, Reichert M, Günes C, Bolenz C, Kuhn F, Maléth J, Speier S, Liebau S, Sipos B, Kuster B, Seufferlein T, Rad R, Meier M, Hohwieler M & Kleger A (2021). Modeling plasticity and dysplasia of pancreatic ductal organoids derived from human pluripotent stem cells. *Cell Stem Cell* **28**, 1105–1124.e19.
- Bruen C, Miller J, Wilburn J, Mackey C, Bollen TL, Stauderman K & Hebbbar S (2021). Auxora for the treatment of patients with acute pancreatitis and accompanying systemic inflammatory response syndrome: clinical development of a calcium release-activated calcium channel inhibitor. *Pancreas* **50**, 537–543.
- Criddle DN, McLaughlin E, Murphy JA, Petersen OH & Sutton R (2007). The pancreas misled: signals to pancreatitis. *Pancreatology* **7**, 436–446.
- Criddle DN, Murphy J, Fistetto G, Barrow S, Tepikin AV, Neoptolemos JP, Sutton R & Petersen OH (2006). Fatty acid ethyl esters cause pancreatic calcium toxicity via inositol trisphosphate receptors and loss of ATP synthesis. *Gastroenterology* **130**, 781–793.
- Criddle DN, Raraty MGT, Neoptolemos JP, Tepikin AV, Petersen OH & Sutton R (2004). Ethanol toxicity in pancreatic acinar cells: mediation by nonoxidative fatty acid metabolites. *Proc Natl Acad Sci U S A* **101**, 10738–10743.
- Dimagno MJ, Lee S-H, Hao Y, Zhou S-Y, McKenna BJ & Owyang C (2005). A proinflammatory, antiapoptotic phenotype underlies the susceptibility to acute pancreatitis in cystic fibrosis transmembrane regulator (−/−) mice. *Gastroenterology* **129**, 665–681.
- Fanczal J, Pallagi P, Görög M, Diszházi G, Almássy J, Madácsy T, Varga Á, Csernay-Biró P, Katona X, Tóth E, Molnár R, Rakonczay Z, Hegyi P & Maléth J (2020). TRPM2-mediated extracellular Ca<sup>2+</sup> entry promotes acinar cell necrosis in biliary acute pancreatitis. *J Physiol* **598**, 1253–1270.
- Freedman SD, Kern HF & Scheele GA (2001). Pancreatic acinar cell dysfunction in CFTR<sup>−/−</sup> mice is associated with impairments in luminal pH and endocytosis. *Gastroenterology* **121**, 950–957.
- Gerasimenko JV, Flowerdew SE, Voronina SG, Sukhomlin TK, Tepikin AV, Petersen OH & Gerasimenko OV (2006). Bile acids induce Ca<sup>2+</sup> release from both the endoplasmic reticulum and acidic intracellular calcium stores through activation of inositol trisphosphate receptors and ryanodine receptors. *J Biol Chem* **281**, 40154–40163.
- Gerasimenko JV, Gryshchenko O, Ferdek PE, Stapleton E, Hébert TOG, Bychkova S, Peng S, Begg M, Gerasimenko OV & Petersen OH (2013). Ca<sup>2+</sup> release-activated Ca<sup>2+</sup> channel blockade as a potential tool in anti-pancreatitis therapy. *Proc Natl Acad Sci U S A* **110**, 13186–13191.
- Hegyi P, Pandol S, Venglovecz V & Rakonczay Z (2011). The acinar-ductal tango in the pathogenesis of acute pancreatitis. *Gut* **60**, 544–552.
- Hong JH, Li Q, Kim MS, Shin DM, Feske S, Birnbaumer L, Cheng KT, Ambudkar IS & Muallem S (2011). Polarized but differential localization and recruitment of STIM1, Orai1 and TRPC channels in secretory cells. *Traffic* **12**, 232–245.
- Huang W, Booth DM, Cane MC, Chvanov M, Javed MA, Elliott VL, Armstrong JA, Dingsdale H, Cash N, Li Y, Greenhalf W, Mukherjee R, Kaphalia BS, Jaffar M, Petersen OH, Tepikin AV, Sutton R & Criddle DN (2014). Fatty acid ethyl ester synthase inhibition ameliorates ethanol-induced Ca<sup>2+</sup>-dependent mitochondrial dysfunction and acute pancreatitis. *Gut* **63**, 1313–1324.
- Jha A, Ahuja M, Maléth J, Moreno CM, Yuan JP, Kim MS & Muallem S (2013). The STIM1 CTID domain determines access of SARAF to SOAR to regulate Orai1 channel function. *J Cell Biol* **202**, 71–79.
- Kim JY, Kim KH, Lee JA, Namkung W, Sun A-Q, Ananthanarayanan M, Suchy FJ, Shin DM, Muallem S & Lee MG (2002). Transporter-mediated bile acid uptake causes Ca<sup>2+</sup>-dependent cell death in rat pancreatic acinar cells. *Gastroenterology* **122**, 1941–1953.
- Kim MS, Hong JH, Li Q, Shin DM, Abramowitz J, Birnbaumer L & Muallem S (2009). Deletion of TRPC3 in mice reduces store-operated Ca<sup>2+</sup> influx and the severity of acute pancreatitis. *Gastroenterology* **137**, 1509–1517.
- Kim MS, Lee KP, Yang D, Shin DM, Abramowitz J, Kiyonaka S, Birnbaumer L, Mori Y & Muallem S (2011). Genetic and pharmacologic inhibition of the Ca<sup>2+</sup> influx channel TRPC3 protects secretory epithelia from Ca<sup>2+</sup>-dependent toxicity. *Gastroenterology* **140**, 2107–2115.e4.
- Krüger B, Albrecht E & Lerch MM (2000). The role of intracellular calcium signaling in premature protease activation and the onset of pancreatitis. *Am J Pathol* **157**, 43–50.
- Lur G, Haynes LP, Prior IA, Gerasimenko OV, Feske S, Petersen OH, Burgoyne RD & Tepikin AV (2009). Ribosome-free terminals of rough ER allow formation of STIM1 puncta and segregation of STIM1 from IP<sub>3</sub> receptors. *Curr Biol* **19**, 1648–1653.
- Madácsy T, Pallagi P & Maleth J (2018). Cystic fibrosis of the pancreas: The role of CFTR channel in the regulation of intracellular Ca<sup>2+</sup> signaling and mitochondrial function in the exocrine pancreas. *Front Physiol* **9**, 1585.
- Maléth J, Balázs A, Pallagi P, Balla Z, Kui B, Katona M, Judák L, Németh I, Kemény LV, Jr ZR, Venglovecz V, Földesi I, Pető Z, Somorác Á, Borka K, Perdomo D, Lukacs GL, Gray MA, Monterisi S, Zaccolo M, Sandler M, Mayerle J, Kühn J-P, Lerch MM, Sahin-Tóth M & Hegyi P (2015). Alcohol disrupts levels and function of the cystic fibrosis transmembrane conductance regulator to promote development of pancreatitis. *Gastroenterology* **148**, 427–439.e16.
- Maléth J & Hegyi P (2014). Calcium signaling in pancreatic ductal epithelial cells: an old friend and a nasty enemy. *Cell Calcium* **55**, 337–345.
- Maléth J & Hegyi P (2016). Ca<sup>2+</sup> toxicity and mitochondrial damage in acute pancreatitis: translational overview. *Philos Trans R Soc Lond B Biol Sci* **371**, 20150425.

- Maléth J, Venglovecz V, Rázga Z, Tiszlavicz L, Rakonczay Z & Hegyi P (2011). Non-conjugated chenodeoxycholate induces severe mitochondrial damage and inhibits bicarbonate transport in pancreatic duct cells. *Gut* **60**, 136–138.
- Molnár R, Madácsy T, Varga Á, Németh M, Katona X, Görög M, Molnár B, Fanczal J, Rakonczay Z, Hegyi P, Pallagi P & Maléth J (2020). Mouse pancreatic ductal organoid culture as a relevant model to study exocrine pancreatic ion secretion. *Lab Invest* **100**, 84–97.
- Pallagi P, Balla Z, Singh AK, Dósa S, Iványi B, Kukor Z, Tóth A, Riederer B, Liu Y, Engelhardt R, Jármay K, Szabó A, Janovszky A, Perides G, Venglovecz V, Maléth J, Wittmann T, Takács T, Gray MA, Gácsér A, Hegyi P, Seidler U & Rakonczay Z Jr (2014). The role of pancreatic ductal secretion in protection against acute pancreatitis in mice. *Crit Care Med* **42**, e177–e188.
- Pallagi P, Madácsy T, Varga Á & Maléth J (2020). Intracellular  $Ca^{2+}$  signalling in the pathogenesis of acute pancreatitis: recent advances and translational perspectives. *Int J Mol Sci* **21**, 4005.
- Pallagi P, Venglovecz V, Rakonczay Z, Borka K, Korompay A, Ozsvári B, Judák L, Sahin-Tóth M, Geisz A, Schnúr A, Maléth J, Takács T, Gray MA, Argent BE, Mayerle J, Lerch MM, Wittmann T & Hegyi P (2011). Trypsin reduces pancreatic ductal bicarbonate secretion by inhibiting CFTR  $Cl^-$  channels and luminal anion exchangers. *Gastroenterology* **141**, 2228–2239.e6.
- Párniczky A, Kui B, Szentesi A, Balázs A, Szűcs Á, Mosztbacher D, Czimmer J, Sarlós P, Bajor J, Gódi S, Vincze Á, Illés A, Szabó I, Pár G, Takács T, Czákó L, Szepes Z, Rakonczay Z, Izbéki F, Gervain J, Halász A, Novák J, Crai S, Hritz I, Góg C, Sümegi J, Golovics P, Varga M, Bod B, Hamvas J, Varga-Müller M, Papp Z, Sahin-Tóth M & Hegyi P; Hungarian Pancreatic Study Group (2016). Prospective, multicentre, nationwide clinical data from 600 cases of acute pancreatitis. *PLoS One* **11**, e0165309.
- Perides G, van Acker GJD, Laukkanen JM & Steer ML (2010). Experimental acute biliary pancreatitis induced by retrograde infusion of bile acids into the mouse pancreatic duct. *Nat Protoc* **5**, 335–341.
- Petersen OH, Tepikin AV, Gerasimenko JV, Gerasimenko OV, Sutton R & Criddle DN (2009). Fatty acids, alcohol and fatty acid ethyl esters: toxic  $Ca^{2+}$  signal generation and pancreatitis. *Cell Calcium* **45**, 634–642.
- Son A, Ahuja M, Schwartz DM, Varga A, Swaim W, Kang N, Maleth J, Shin DM & Muallem S (2019).  $Ca^{2+}$  influx channel inhibitor SARAF protects mice from acute pancreatitis. *Gastroenterology* **157**, 1660–1672.e2.
- Swain SM, Romac JM-J, Shahid RA, Pandol SJ, Liedtke W, Vigna SR & Liddle RA (2020). TRPV4 channel opening mediates pressure-induced pancreatitis initiated by Piezo1 activation. *J Clin Invest* **130**, 2527–2541.
- Venglovecz V, Rakonczay Z, Ozsvári B, Takács T, Lonovics J, Varró A, Gray MA, Argent BE & Hegyi P (2008). Effects of bile acids on pancreatic ductal bicarbonate secretion in guinea pig. *Gut* **57**, 1102–1112.
- Voronina S, Longbottom R, Sutton R, Petersen OH & Tepikin A (2002). Bile acids induce calcium signals in mouse pancreatic acinar cells: implications for bile-induced pancreatic pathology. *J Physiol* **540**, 49–55.
- Waldron RT, Chen Y, Pham H, Go A, Su H-Y, Hu C, Wen L, Husain SZ, Sugar CA, Roos J, Ramos S, Lugea A, Dunn M, Stauderman K & Pandol SJ (2019). The Orai  $Ca^{2+}$  channel inhibitor CM4620 targets both parenchymal and immune cells to reduce inflammation in experimental acute pancreatitis. *J Physiol* **597**, 3085–3105.
- Wen L, Voronina S, Javed MA, Awais M, Szatmary P, Latawiec D, Chvanov M, Collier D, Huang W, Barrett J, Begg M, Stauderman K, Roos J, Grigoryev S, Ramos S, Rogers E, Whitten J, Velicelebi G, Dunn M, Tepikin AV, Criddle DN & Sutton R (2015). Inhibitors of ORAI1 prevent cytosolic calcium-associated injury of human pancreatic acinar cells and acute pancreatitis in 3 mouse models. *Gastroenterology* **149**, 481–492.e7.
- Yadav D & Lowenfels AB (2013). The epidemiology of pancreatitis and pancreatic cancer. *Gastroenterology* **144**, 1252–1261.
- Zeng M, Szymczak M, Ahuja M, Zheng C, Yin H, Swaim W, Chiorini JA, Bridges RJ & Muallem S (2017). Restoration of CFTR activity in ducts rescues acinar cell function and reduces inflammation in pancreatic and salivary glands of mice. *Gastroenterology* **153**, 1148–1159.
- Zhu Z-D, Yu T, Liu H-J, Jin J & He J (2018). SOCE induced calcium overload regulates autophagy in acute pancreatitis via calcineurin activation. *Cell Death Dis* **9**, 50.

## Additional information

### Data availability statement

The authors declare that all data supporting the results are included in the paper. There are no shared datasets in this manuscript.

### Competing interests

The authors have no conflict of interest to declare. CalciMedica supplied CM5480 for the study.

### Author contributions

P.P. and J.M. designed the research project; M.G., P.P., T.M., Á.V., N.P., T.C., V.V., A.G., V.S.Z., M.M., K.D. and J.M. contributed to acquisition, analysis and interpretation of data for the work. E.S.Z. and L.G.Y. provided human pancreatic tissue samples. M.G., P.P., T.M., Á.V., R.Z., H.P. and J.M. drafted the work and all authors approved the final version of the manuscript, agree to be accountable for all aspects of the work in ensuring that questions related to the accuracy or integrity of any part of the work are appropriately investigated and resolved. All persons designated as authors qualify for authorship, and all those who qualify for authorship are listed.

## Funding

The research was supported by funding from the Hungarian National Research, Development and Innovation Office (GINOP-2.3.2-15-2016-00048 to J.M., PD116553 to P.P.), the Ministry of Human Capacities (EFOP 3.6.2-16-2017-00006 to J.M.), Bolyai Research Fellowship (BO/00569/17 to P.P.), the Hungarian Academy of Sciences (LP2017-18/2017 to J.M.), the National Excellence Programme (20391-3/2018/FEKUSTRAT, TUDFO/47138-1/2019/ITM, TKP2020 and TKP2021-EGA-28 to J.M.), and the New National Excellence Program of the Ministry of Human Capacities (ÚNKP-21-4-SZTE-1116 to T.M. and ÚNKP-21-3-SZTE-68 to N.P. This work was also supported by Albert Szent-Györgyi Research Grant (to T.C. ) by the Faculty of Medicine, University of Szeged. The project has also received funding from the EU's Horizon 2020 research and innovation programme under grant agreement No. 739593. Current work

was also supported by funding from the Hungarian Government (NTP-NFTÖ-B-0011 to Á.V. and NTP-NFTÖ-21-B-0079 to V.Sz.)

## Keywords

acute pancreatitis, bile acid, Ca<sup>2+</sup> signalling, epithelial ion transport, ethanol, Orail channel

## Supporting information

Additional supporting information can be found online in the Supporting Information section at the end of the HTML view of the article. Supporting information files available:

## Peer Review History

## Statistical Summary Document